Pharmacological Research 214 (2025) 107682

Contents lists available at ScienceDirect

Pharmacological Research

journal homepage: www.elsevier.com/locate/yphrs

CB_1 cannabinoid receptor agonists induce acute respiratory depression in awake mice☆

Joshua Watkins [a,b], Petra Aradi [a], Rachel Hahn [a], Alexandros Makriyannis [c], Ken Mackie [a,b,d], Istvan Katona [a,b,e], Andrea G. Hohmann [a,b,d,*]

[a] Department of Psychological and Brain Sciences, Indiana University Bloomington, Bloomington, IN 47405, United States
[b] Program in Neuroscience, Indiana University Bloomington, Bloomington, IN 47405, United States
[c] Center for Drug Discovery, Northeastern University, Boston, MA 02115, United States
[d] Gill Institute for Neuroscience, Indiana University, Bloomington, IN 47405, United States
[e] Institute of Experimental Medicine, HUN-REN, Budapest, Hungary

ARTICLE INFO

Keywords:
Respiratory depression
Cannabinoid
Overdose
Pre-Botzinger complex
Opioid
THC

ABSTRACT

Recreational use of synthetic cannabinoid agonists (i.e., "spice compounds") that target the cannabinoid type 1 receptor (CB_1) can cause acute respiratory failure in humans. However, Δ^9-tetrahydrocannabinol (Δ^9-THC), the major psychoactive phytocannabinoid in cannabis, is not traditionally thought to interact with the brain respiratory system, based largely upon sparse labeling of CB_1 receptors in the medulla and relative safety suggested by widespread human use. Here we used whole body plethysmography and RNAscope *in situ* hybridization in mice to reconcile this conflict between conventional wisdom and human data. We examined the respiratory effects of the synthetic CB_1 full agonist CP55,940 and Δ^9-THC in male and female mice. CP55,940 and Δ^9-THC potently and dose-dependently suppressed minute ventilation and tidal volume, decreasing measures of respiratory effort (i.e., peak inspiratory and expiratory flow). Both cannabinoids reduced respiratory frequency, decreasing inspiratory and expiratory time while markedly increasing inspiratory and expiratory pause. Respiratory suppressive effects were fully blocked by the CB_1 antagonist AM251, were minimally impacted by the peripherally-restricted CB_1 antagonist AM6545, and occurred at doses lower than those that produce cardinal behavioral signs of CB_1 activation. Using RNAscope *in situ* hybridization, we also demonstrated extensive coexpression of *Cnr1* (encoding the CB_1 receptor) and *Oprm1* (encoding the μ-opioid receptor) mRNA in respiratory cells in the medullary pre-Bötzinger complex, a critical nucleus of respiratory control. Our results show that mRNA for CB_1 is present in respiratory cells in a medullary brain region essential for breathing and demonstrate that cannabinoids produce respiratory suppression via activation of central CB_1 receptors.

1. Introduction

There are no reports of human cannabis use leading to death by respiratory depression. As respiratory depression is the main cause of death in drug overdose [1], this lack of lethal cannabis overdoses has led to the perception that cannabinoids do not inhibit respiratory drive. This perception is bolstered by sparse levels of cannabinoid receptor binding in the medulla, where breathing is primarily controlled [2].

This perception of relative safety has been challenged by the emergence of illicit synthetic cannabinoids. Whereas Δ^9-tetrahydrocannabinol (Δ^9-THC), the main psychoactive component of cannabis, is a weak partial agonist of the Cannabinoid Type 1 (CB_1) receptor [3–5], synthetic compounds are typically high-potency, high-efficacy CB_1 agonists [6,7] that are sold under generic names (e.g., "Spice," "K2," "synthetic marijuana") and marketed as legal or more potent alternatives to cannabis. Users of illicit synthetic cannabinoids can experience acute respiratory failure requiring emergency medical care [8–13] and synthetic cannabinoids have also been detected in lethal opioid

☆ This article is co-authored by an editorial Board Member. According to our policy the article has been handled by another editor independently, with the authors being blind to the whole process.

* Correspondence to: Department of Psychological and Brain Sciences, Gill Institute for Neuroscience, Indiana University, 1101 E. 10th Street, Bloomington, IN 47405-7007, USA.
E-mail address: hohmanna@iu.edu (A.G. Hohmann).

https://doi.org/10.1016/j.phrs.2025.107682
Received 12 January 2025; Received in revised form 28 February 2025; Accepted 1 March 2025
Available online 8 March 2025

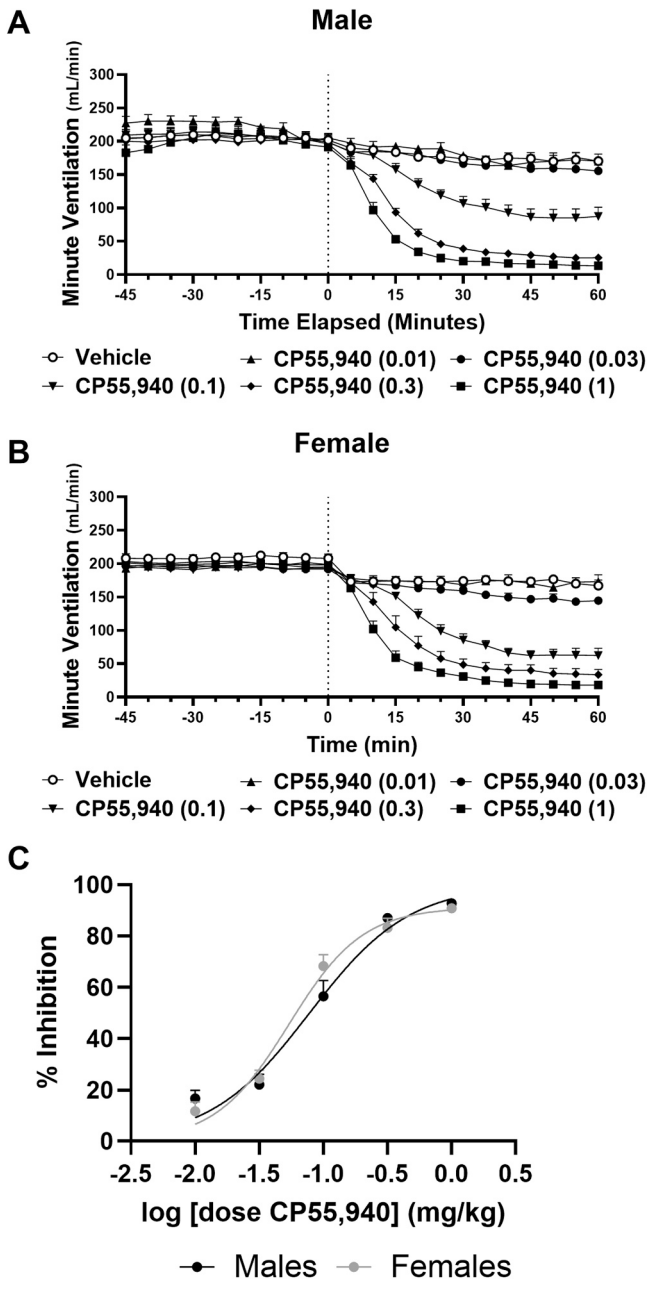

Fig. 1. CP55,940 reduces minute ventilation in mice of both sexes. CP55,940 reduces minute ventilation in a dose- and time-dependent manner in both (**A**) male and (**B**) female mice at doses of 0.1 mg/kg i.p. and higher (Tables 1 and 2). (**A-B**) Data were analyzed by Two-way ANOVA, Dunnett's *post hoc* test, $p < 0.05$ considered significant. $p < 0.0001$ for all active doses vs. vehicle. (**C**) Dose response of CP55,940 suppressing minute ventilation in male and female mice. ED_{50} (95 % CI): Males: 0.078 (0.057 – 0.095) mg/kg i.p.; Females: 0.054 (0.043 – 0.070) mg/kg i.p. Data are Mean ± SEM (where visible) derived from n = 6–8 mice per group.

overdose [14,15]. This emerging clinical literature requires that the effects of cannabinoids on respiration and the distribution of cannabinoid receptors within respiratory circuits be reevaluated using the most sensitive techniques available.

Existing literature on the respiratory effects of CB_1 agonists is fragmented, conflicting, and includes non-standard [16] dependent measures (for review see Wiese et al., 2023 [17]). Early literature employed thoracic transducers [18,19], which are imprecise by modern standards and limited to observations of respiratory rate, and assessed respiratory parameters in anesthetized, tracheotomized, or mechanically ventilated animals, limiting extrapolation to awake behaving animals and humans. The few existing studies that have measured both respiratory rate and amplitude report conflicting results on both metrics [20,21]. Studies utilizing the current standard for recording respiratory activity - whole body plethysmography in awake animals - only report effects on respiratory frequency [22] or assess CB_2-opioid interactions [23]. We, consequently, evaluated the ability of the synthetic CB_1 cannabinoid full agonist CP55,940 and CB_1 partial agonist Δ^9-THC to produce respiratory depression in awake, unrestrained C57Bl/6 J mice using whole body plethysmography. Pharmacological specificity was assessed using both brain penetrant (AM251) and peripherally-restricted (AM6545) CB_1 antagonists.

The pre-Bötzinger complex is a brain region critical to respiration [24–26]. Suppression of excitatory signaling in the pre-Bötzinger complex reduces rhythmic inspiration, leading to infrequent low amplitude breathing and sustained interruptions to the respiratory cycle [27]. The pre-Bötzinger complex is critically (though not solely) implicated in the respiratory suppressive effects of exogenous opioids; application of the μ-opioid receptor (MOR) antagonist naloxone into the pre-Bötzinger complex prevents fentanyl-induced respiratory depression at astoundingly low doses in animal models, and MOR deletion in the pre-Bötzinger complex attenuates respiratory rate depression by morphine [28–31]. We therefore asked whether *Cnr1* mRNA (encoding the CB_1 receptor) was expressed in the pre-Bötzinger complex using RNAscope *in situ* hybridization and identified phenotypes of respiratory cells expressing *Cnr1* expression in this region.

Here we show that the prototypical cannabinoid agonists CP55,940 and Δ^9-THC induce CB_1-mediated respiratory depression in awake adult mice of both sexes after systemic (IP) injection. We further demonstrate extensive overlap between respiratory cells expressing *Cnr1* mRNA and *Oprm1* mRNA, suggesting that respiratory depression induced by CB_1 agonists may share cellular sites of action with the respiratory effects of drugs that activate MOR.

2. Materials and methods

2.1. Animals

Subjects consisted of 126 male and 60 female C57BL/6 J wild type mice (Jackson Laboratories; Bar Harbor, ME) 12 weeks of age at time of testing. Naive male CD1 (n = 3) wild type and $CB_1^{-/-}$ mice (n = 3) on a CD1 background strain were used in RNAscope experiments at 12 weeks of age. Male mice weighed 30–40 g, and female mice weighed 19–30 g prior to testing. Mice were housed in a temperature- and humidity-controlled facility with *ad libitum* access to food and water on a 12:12 h light/dark cycle. All procedures were approved by the Bloomington Institutional Animal Care and Use Committee of Indiana University. All experiments comply with the standards set in the Association for Assessment and Accreditation of Laboratory Animal Care (AAALAC) Guide for the Care and Use of Laboratory Animals, the World Medical Association Statement on Animal Use in Biomedical Research, and the European Union Directive on the Protection of Animals used for Scientific Purposes.

2.2. Drugs

CP55,940 was purchased from Cayman Pharmaceuticals (Ann Arbor, MI). Δ^9-THC was obtained from the NIDA Drug Supply Program (Division of Therapeutics and Medical Consequences, National Institutes of Health). AM251 and AM6545 were synthesized by the Makriyannis laboratory (Northeastern University, Boston, MA). All drugs used in pharmacological experiments were administered intraperitoneally in a volume of 10 mL/kg. Drugs were administered in a vehicle consisting of 10 % dimethyl sulfoxide (DMSO; Sigma-Aldrich, St. Louis, MO) with the remaining volume consisting of emulphor (Alkamuls EL-620; Solvay), 100 % ethanol (Decon Labs; Montgomery, PA), and 0.9 % saline (Baxter

Table 1
Statistical analysis of the respiratory effects of CP55,940 in male mice.

Metric	Time		Drug		Interaction		Effective Doses (mg/kg)				
	F	p	F	p	F	p	0.01	0.03	0.1	0.3	1
MV	$F_{11,363} = 212.7$	0.0001	$F_{5,33} = 86.10$	0.0001	$F_{55,363} = 23.28$	0.0001	-	-	0.0001	0.0001	0.0001
Vt	$F_{11,363} = 129.9$	0.0001	$F_{5,33} = 41.67$	0.0001	$F_{55,363} = 17.73$	0.0001	-	-	0.0200	0.0001	0.0001
PIF	$F_{11,363} = 130.7$	0.0001	$F_{5,33} = 74.70$	0.0001	$F_{55,363} = 16.46$	0.0001	-	-	0.0001	0.0001	0.0001
PEF	$F_{11,363} = 192.0$	0.0001	$F_{5,33} = 52.94$	0.0001	$F_{55,363} = 17.85$	0.0001	-	-	0.0001	0.0001	0.0001
Fr	$F_{11,363} = 249.5$	0.0001	$F_{5,33} = 163.5$	0.0001	$F_{55,363} = 38.21$	0.0001	-	-	0.0001	0.0001	0.0001
Ti	$F_{11,363} = 120.1$	0.0001	$F_{5,33} = 120.6$	0.0001	$F_{55,363} = 34.85$	0.0001	-	-	0.0015	0.0001	0.0001
Te	$F_{11,363} = 58.91$	0.0001	$F_{5,33} = 138.9$	0.0001	$F_{55,363} = 23.70$	0.0001	-	-	-	0.0001	0.0001
EIP	$F_{11,363} = 93.73$	0.0001	$F_{5,33} = 185.9$	0.0001	$F_{55,363} = 46.67$	0.0001	-	-	-	0.0001	0.0001
EEP	$F_{11,363} = 15.37$	0.0001	$F_{5,33} = 29.58$	0.0001	$F_{55,363} = 13.00$	0.0001	-	-	-	-	0.0001

Data were analyzed by Two-way repeated measures ANOVA followed by Dunnett's *post hoc* test. $P < 0.05$ considered significant. Abbreviations: MV, Minute Ventilation; Vt, Tidal Volume; PIF, Peak Inspiratory Flow; PEF, Peak Expiratory Flow; Fr, Frequency; Ti, Inspiratory Time; Te, Expiratory Time; EIP, End Inspiratory Pause; EEP, End Expiratory Pause.

Table 2
Statistical analysis of the respiratory effects of CP55,940 in female mice.

Metric	Time		Drug		Interaction		Effective Doses (mg/kg)				
	F	p	F	p	F	p	0.01	0.03	0.1	0.3	1
MV	$F_{11,352} = 257.1$	0.0001	$F_{5,32} = 69.77$	0.0001	$F_{55,352} = 41.31$	0.0001	-	-	0.0001	0.0001	0.0001
Vt	$F_{11,352} = 157.8$	0.0001	$F_{5,32} = 46.01$	0.0001	$F_{55,352} = 28.81$	0.0001	-	-	0.0001	0.0001	0.0001
PIF	$F_{11,352} = 157.4$	0.0001	$F_{5,32} = 79.26$	0.0001	$F_{55,352} = 32.15$	0.0001	-	0.0235	0.0001	0.0001	0.0001
PEF	$F_{11,352} = 239.7$	0.0001	$F_{5,32} = 45.13$	0.0001	$F_{55,352} = 29.55$	0.0001	-	-	0.0001	0.0001	0.0001
Fr	$F_{11,352} = 232.5$	0.0001	$F_{5,32} = 60.36$	0.0001	$F_{55,352} = 36.43$	0.0001	-	-	0.0001	0.0001	0.0001
Ti	$F_{11,352} = 53.36$	0.0001	$F_{5,32} = 31.51$	0.0001	$F_{55,352} = 12.32$	0.0001	-	-	0.0071	0.0001	0.0001
Te	$F_{11,352} = 33.42$	0.0001	$F_{5,32} = 17.41$	0.0001	$F_{55,352} = 9.325$	0.0001	-	-	-	0.0016	0.0001
EIP	$F_{11,352} = 34.38$	0.0001	$F_{5,32} = 18.89$	0.0001	$F_{55,352} = 12.20$	0.0001	-	-	-	0.0055	0.0001
EEP	$F_{11,352} = 4.371$	0.0001	$F_{5,32} = 7.693$	0.0001	$F_{55,352} = 4.371$	0.0001	-	-	-	-	0.0001

Data were analyzed by Two-way repeated measures ANOVA followed by Dunnett's *post hoc* test. $P < 0.05$ considered significant. Abbreviations: MV, Minute Ventilation; Vt, Tidal Volume; PIF, Peak Inspiratory Flow; PEF, Peak Expiratory Flow; Fr, Frequency; Ti, Inspiratory Time; Te, Expiratory Time; EIP, End Inspiratory Pause; EEP, End Expiratory Pause.

Pharmaceuticals; Bloomington, IN) in a 1:1:18 ratio. Due to limited solubility in experiments involving both CP55,940 and AM6545, all drugs were administered in a vehicle consisting of 20 % DMSO with the remaining volume consisting of emulphor, ethanol, and saline in a 1:1:18 ratio.

2.3. Assessment of respiratory parameters

Whole body plethysmography (Data Sciences International; St. Paul, MN) was used to assess respiratory parameters in awake and unrestrained mice. Respiratory parameters evaluated were respiratory frequency (breaths per minute (min)), tidal volume (volume of individual breaths), minute ventilation (volume of ventilation in mL/min), total inspiratory time (ms), total expiratory time (ms), peak inspiratory flow (mL/sec), peak expiratory flow (mL/sec), end inspiratory pause (time between inspiration and expiration; ms), and end expiratory pause (time between respiratory cycles; ms). Mice were habituated to recording chambers for 30 minutes within 48 hours of testing to minimize changes in respiration resulting from exploratory behavior or stress related to a novel environment. On the test day, mice received air mixed with 10 % CO_2 to standardize hypercapnic responses. Testing consisted of a 50-minute initial recording to acquire baseline respiratory parameters, after which mice were briefly removed from test chambers and given a single IP injection of drug or vehicle. Mice were then immediately returned to the chambers for 60 minutes to obtain post-dose respiratory parameters.

Plethysmography was used to evaluate the respiratory effects of the synthetic CB_1 cannabinoid full agonist CP55,940 and the CB_1 partial agonist Δ^9-THC. Respiratory parameters were measured before (i.e. baseline) and after a single i.p. injection of CP55,940 (0.01, 0.03, 0.1, 0.3, or 1 mg/kg) or vehicle in male and female mice (n = 6–8 per group). Respiratory parameters were similarly measured before and after a single i.p. injection of Δ^9-THC (0.3, 1, 3, 10, or 30 mg/kg) or vehicle in mice of both sexes (n = 6–8 per group). We also assessed pharmacological specificity and the role of central CB_1 receptors in the respiratory effects of CP55,940 and Δ^9-THC using male mice. Respiratory parameters were measured before and after injection of either the CNS-penetrant CB_1 inverse agonist AM251 (5 mg/kg) or the peripherally restricted CB_1 antagonist AM6545 (10 mg/kg) administered either alone or coadministered with either CP55,940 (0.3 mg/kg, i.p.) or Δ^9-THC (10 mg/kg, i.p.) (n = 6–8 per group). Injection volumes were equated in all studies. Testing of vehicle, doses and agonist-antagonist coadministration conditions were interleaved. No mouse received more than one drug dose or pharmacological manipulation in any experiment.

2.4. Perfusion and sectioning

Naive male CD1 wild type (n = 3) and $CB_1^{-/-}$ (n = 3) mice (postnatal day 84) were deeply anesthetized with isoflurane (Covetrus, Portland, ME) and perfused transcardially with 0.9 % saline for two minutes, followed by 4 % paraformaldehyde (PFA, Sigma, P6148) dissolved in 0.1 M phosphate buffer (PB, pH 7.4 containing Na_2HPO_4S, Sigma, 71–500) for 18 minutes using approximately 5 mL/min pump speed. After perfusion, brains were removed from the skull and postfixed at room temperature overnight in 4 % PFA. Then, 40 µm coronal sections (5 sections total derived from 3 WT mice; 3 sections derived from 3 $CB_1^{-/-}$ mice) were cut in PB using a Leica VT-1200S vibratome (Nussloch, Germany). Landmarks used to determine section level were the appearance of the 4th ventricle, the presence of white matter tracts in the 6th cerebellar lobule, and the disappearance of both the central canal and *area postrema*, consistent with figures 88 through 90 (corresponding to −6.84 to −7.08 mm bregma) in The Mouse Brain in Stereotaxic Coordinates, 3rd Edition [32]. All solutions were prepared from filtered water distilled through a Biopak Polisher (Sigma, CDUFBI001)

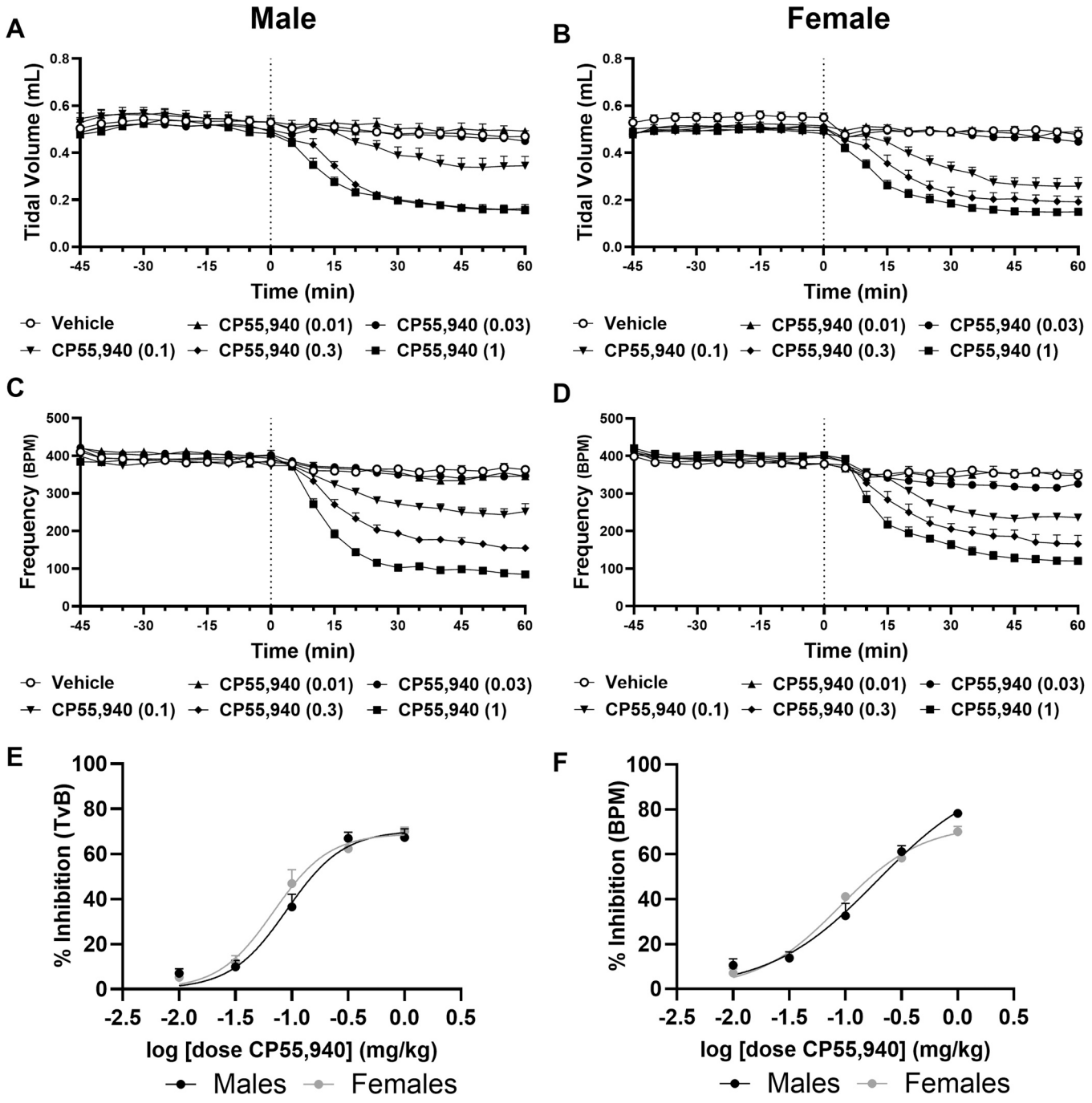

Fig. 2. CP55,940 reduces tidal volume and respiratory frequency in mice of both sexes. CP55,940 reduced tidal volume in a dose- and time-dependent manner in (**A**) male and (**B**) female mice (see Tables 1–2) at doses of 0.1 mg/kg i.p. and higher. CP55,940 similarly reduces frequency in both (**C**) male and (**D**) female mice. Respiratory frequency was significantly suppressed by i.p. doses 0.1 mg/kg and above in both males (Table 1) and females (Table 2). **(E)** Dose response of CP55,940 in suppressing tidal volume in male and female mice. ED_{50} (95 % CI): Males: 0.91 (0.069 – 0.125) mg/kg i.p.; Females: 0.69 (0.052 – 0.098) mg/kg i.p. **(F)** Dose response of CP55,940 in suppressing respiratory frequency in male and female mice. ED_{50} (95 % CI): Males: 0.193 (0.112 – 0.259) mg/kg i.p.; Females: 0.089 (0.063 – 0.155) mg/kg i.p. (**A-D**) Data are expressed as Mean ± SEM (where visible) derived from n = 6–8 mice per group. Data are analyzed by Two-way ANOVA, Dunnett's *post hoc* test, $p < 0.05$ considered significant. All active doses $p < 0.0200$ vs. vehicle. Statistical results are detailed in Tables 1 and 2.

to decrease RNase contamination.

2.5. Multiplex fluorescent in situ hybridization

RNAscope *in situ* hybridization was used to detect mRNA encoding the CB_1 receptor. Specificity of the signal was assessed using brain sections derived from $CB_1^{-/-}$ mice that were sectioned and treated in parallel with sections obtained from wild-type mice. Tissue sections were mounted on positively- charged microscopic Superfrost Plus slides (Fisher Scientific, Waltham, MA), then a series of dehydration steps were performed using 50 %, 70 %, and 100 % ethanol (Sigma, E7023). Sections were incubated in 100 % ethanol overnight at 4°C. The next day, the sections were dried, and a barrier was drawn around the slices with a hydrophobic pen (ImmEdge Hydrophobic Barrier, Vector Laboratories). RNAscope mRNA-labeling steps were performed following the manufacturer's protocols. The sections were coverslipped with fluorescent

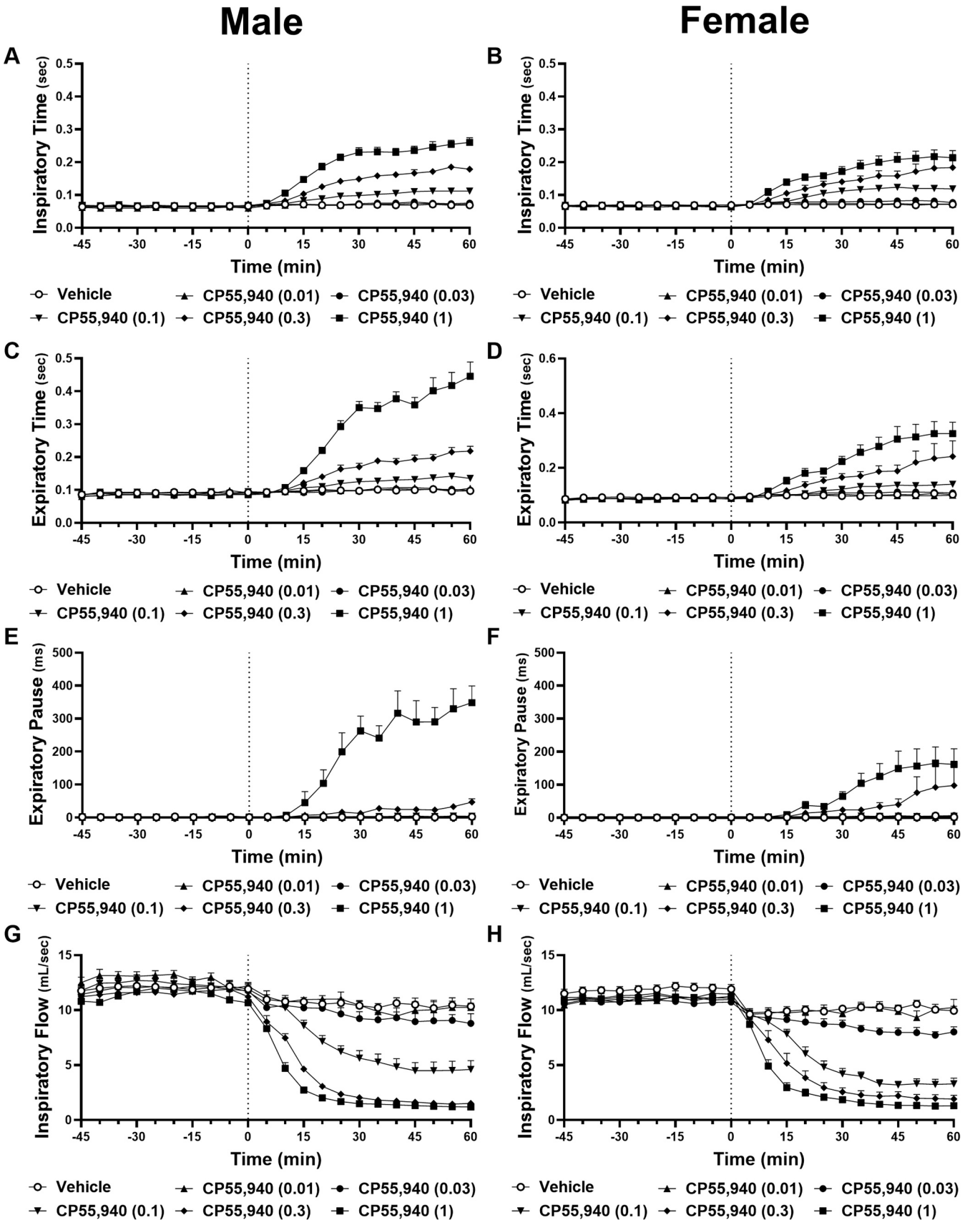

(caption on next page)

Fig. 3. CP55,940 prolongs inspiratory and expiratory time as well as inspiratory and expiratory pause in mice of both sexes. CP55,940 prolongs inspiratory time in both (**A**) male and (**B**) female mice at all doses 0.1 mg/kg and above in both sexes (Tables 1 and 2). Expiratory time was similarly increased in both (**C**) male and (**D**) female mice at all i.p. doses 0.3 mg/kg and above in both sexes (Tables 1 and 2). Expiratory pause was extended in both (**E**) male and (**F**) female mice; however, only the highest tested dose of 1 mg/kg extended expiratory pause in both males (Table 1) and females (Table 2). CP55,940 reduces inspiratory flow in a time- and dose-dependent manner in both (**G**) male and (**H**) female mice. Inspiratory flow was suppressed by doses of CP55,940 (i.p.) 0.1 mg/kg and above in males (Table 1) and doses 0.03 mg/kg and above in females (Table 2). (**A-H**) Data are expressed as Mean ± SEM (where visible) derived from n = 6–8 mice per group. Data are analyzed by Two-way ANOVA, Dunnett's *post hoc* test, $p < 0.05$ considered significant. All active doses $p < 0.0071$ vs. vehicle. Statistical results are detailed in Tables 1 and 2. Modest but reliable differences were observed in baseline recordings of the expiratory time of male ($p = 0.0315$) and female (0.0093) mice. *Post hoc* tests did not reveal differences between any specific groups in male mice. In female mice, modest but reliable baseline differences were observed between the vehicle group and the 0.3 mg/kg group ($p = 0.032$) and the vehicle group and 1 mg/kg group ($p = 0.0146$). No differences between groups were observed at the time of injection.

mounting medium (ProLong Diamond Antifade Reagent P36961; Invitrogen, Waltham, MA) and imaged with a Nikon A1 confocal laser-scanning microscope. Sections were imaged with both 20x and 60x objectives to obtain both single-plane images and high-resolution z-stacks of the pre-Bötzinger complex.

Gene-specific RNAscope probes were designed and provided by Advanced Cell Diagnostics (Newark, CA) and used to target the following mRNA sequences: CB_1 (catalog #530–1458, targeting base pairs 530–1458 of the mouse *Cnr1* sequence, NM_007726.3), Nk1r (catalog #428781-C2, targeting base pairs 845–1775 of the mouse *Tacr1* sequence, NM_009313.5) and Mor1 (catalog #315841-C3, targeting base pairs 1135–2162 of the mouse *Oprm1* sequence, NM_001039652.1).

Levels of mRNA expression were quantified by QuPath (v.0.5.1) subcellular detection analysis. All quantification was performed on single-plane images with identical detection thresholds across all samples. The area quantified corresponded to the pre-Bötzinger complex as defined in The Mouse Brain in Stereotaxic Coordinates, 3rd Edition [32].

2.6. Data analysis

All statistics were calculated using GraphPad Prism v.10.2 (GraphPad Software; Boston, MA). Plethysmography data were averaged into five-minute bins and represented as Mean ± SEM where error was large enough to be visually rendered. Two-way repeated measures ANOVA was used to assess the respiratory effects of all pharmacological manipulations across time, and to compare pre-injection baseline responsiveness between groups. Dunnett's *post hoc* test was used to compare main effects of drug treatment with vehicle controls. Bonferroni's *post hoc* test was used to assess the impact of antagonist treatments on respiratory parameters and ascertain whether baseline respiratory parameters differed between treatment groups prior to pharmacological manipulations. Pre-injection and post-injection respiratory parameters were analyzed separately to ensure that differences in baseline responsiveness, if observed, did not impact interpretation of drug effects. Dose response curves were generated by taking the difference between the final pre- and post-dose bin and fitting a four-parameter logistic regression model using Graphpad Prism v.10.2. Model-fitting was constrained to values between zero and one hundred, as negative values (e.g. negative respiratory activity) are not conceptually possible. Bottom values for model-fitting were constrained to zero, as the lowest tested doses in each experiment did not significantly differ from vehicle controls for any metric in any experiment.

3. Results

3.1. General results

Prior to pharmacological manipulations, baseline respiratory parameters, as expected, showed a modest but significant decline across the pre-injection observation interval ($P < 0.05$ for all experiments). Pre-injection measures of minute ventilation did not differ as a function of group allocation. In general, no group differences in other dependent measures assessing baseline responsiveness were observed as a function of drug allocation overall or persisted immediately prior to drug injection, except where specifically noted. Post-injection, observed respiratory effects of CP55,940 and Δ^9-THC were rapid and persisted across the entire recording session; once depressed, no metric recovered to control levels for the duration of recording. Despite the magnitude and persistence of observed respiratory depression, no fatalities were observed in experimental animals.

3.2. Respiratory effects of CP55,940

CP55,940 markedly decreased minute ventilation relative to vehicle in a dose- and time-dependent manner in mice of both sexes (Drug: $p < 0.0001$; Interaction: $p < 0.0001$ for each sex). *Post hoc* comparisons revealed that all doses 0.1 mg/kg and higher suppressed minute ventilation relative to vehicle in both male (0.1–1 mg/kg, $p < 0.0001$; Fig. 1A; Table 1) and female (0.1–1 mg/kg, $p < 0.0001$; Fig. 1B; Table 2) mice. The ED_{50} (95 % Confidence Interval (CI)) for CP55,940-induced suppression of minute ventilation was 0.078 (0.057 – 0.095) mg/kg in males and 0.054 (0.043 – 0.070) mg/kg in females (Fig. 1C), consistent with similar efficacies observed between sexes.

Suppression of overall respiratory activity was driven by a reduction in both the amplitude of gas exchange of each breath and the number of initiated breaths. CP55,940 suppressed tidal volume relative to vehicle in a dose- and time-dependent manner in both male and female mice (Drug: $p < 0.0001$; Interaction: $p < 0.0001$ for each sex); all doses 0.1 mg/kg and above reduced tidal volume relative to vehicle in both male (0.1 mg/kg, $p = 0.0200$; 0.3–1 mg/kg, $p < 0.0001$; Fig. 2A; Table 1) and female (0.1–1 mg/kg, $p < 0.0001$; Fig. 2B; Table 2) mice.

CP55,940 similarly suppressed respiratory frequency relative to vehicle in a dose- and time-dependent manner in mice of both sexes (Drug: $p < 0.0001$; Interaction: $p < 0.0001$ for each sex). All CP55,940 doses 0.1 mg/kg and above reduced respiratory frequency relative to vehicle in male (0.1–1 mg/kg, $p < 0.0001$; Fig. 2C; Table 1) and female (0.1–1 mg/kg, $p < 0.0001$; Fig. 2D; Table 2) mice. The ED_{50} (95 % CI) for suppression of tidal volume by CP55,940 was 0.91 (0.069 – 0.125) mg/kg in male mice and 0.069 (0.052 – 0.098) mg/kg in female mice (Fig. 2E), wheras the ED_{50} (95 % CI) for suppression of frequency by CP55,940 was 0.193 (0.112 – 0.259) mg/kg in male mice and 0.089 (0.063 – 0.155) mg/kg in female mice (Fig. 2F).

The CP55,940-induced reduction in respiratory frequency was driven by an increase in the length of all respiratory phases, although the doses at which these effects were observed were not uniform. CP55,940 extended inspiratory time relative to vehicle in a dose and time-dependent manner in mice of both sexes (Drug: $p < 0.0001$; Interaction: $p < 0.0001$ for each sex); doses of CP55,940 0.1 mg/kg and higher extended inspiratory time relative to vehicle in both male (0.1 mg/kg, $p = 0.0015$; 0.3–1 mg/kg, $p < 0.0001$; Fig. 3A; Table 1) and female (0.1 mg/kg, $p = 0.0071$; 0.3–1 mg/kg, $p < 0.0001$; Fig. 3B; Table 2) mice. Expiratory time was also extended by CP55,940 relative to vehicle in a dose and time-dependent manner in mice of both sexes (Drug: $p < 0.0001$; Interaction: $p < 0.0001$ for each sex); expiratory time was extended relative to vehicle by CP55,940 doses of 0.3 mg/kg and above in both male (0.3–1 mg/kg, $p < 0.0001$; Fig. 3C; Table 1) and female (0.3 mg/kg, $p = 0.0016$; 1 mg/kg, $p < 0.0001$; Fig. 3D; Table 2) mice. End expiratory pause was also extended relative to vehicle in a dose and time-dependent manner in mice of both sexes (Drug: $p < 0.0001$;

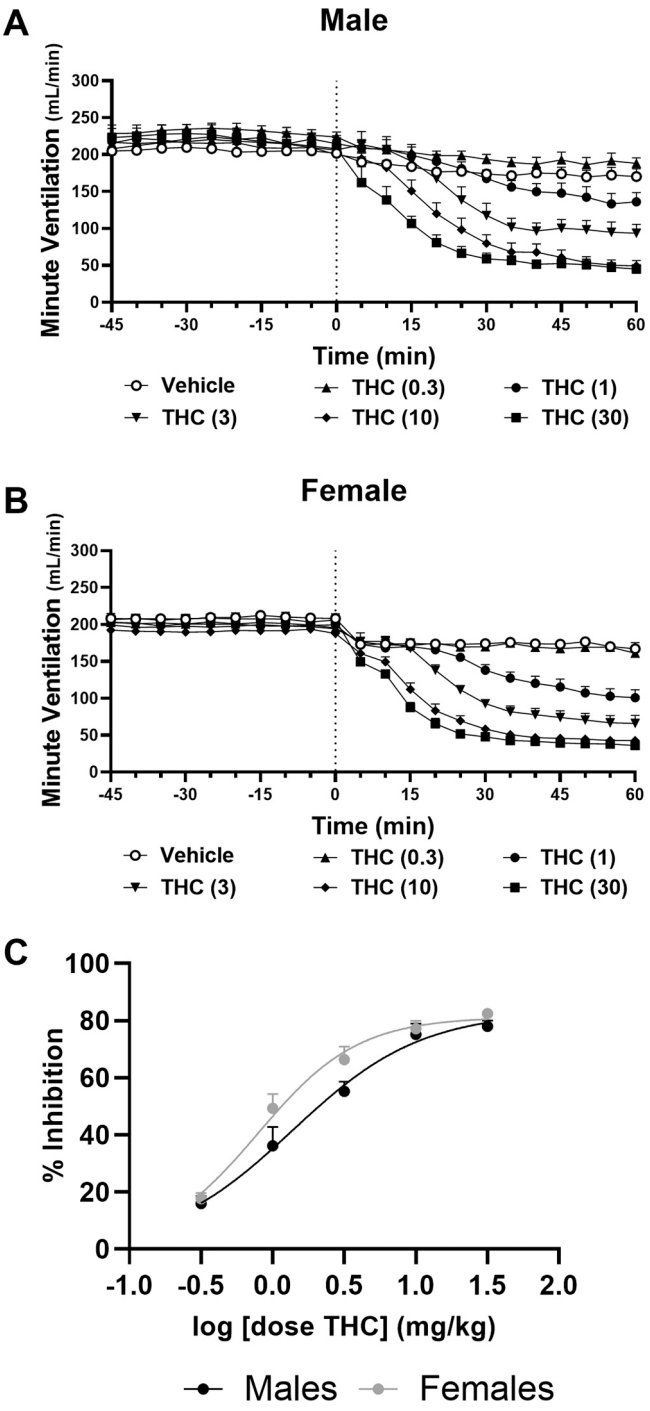

Fig. 4. Δ^9-THC reduces minute ventilation in mice of both sexes. Δ^9-THC reduces minute ventilation in a dose- and time-dependent manner at doses of 3 mg/kg i.p. and higher in (**A**) male mice (Table 3) and doses 1 mg/kg i.p. and higher in (**B**) female mice (Table 4). (**C**) Dose response of Δ^9-THC-induced suppression of minute ventilation in male and female mice. ED_{50} (95 % CI) Males: 1.377 (0.904 – 2.741) mg/kg i.p.; Females: 0.795 (0.606 – 1.109) mg/kg i.p. (**A-B**) Data are expressed as Mean ± SEM (where visible) derived from n = 6–8 mice per group. Data were analyzed by Two-way ANOVA, Dunnett's *post hoc* test, $p < 0.05$ considered significant. All active doses $p < 0.0146$ vs. vehicle. Statistical results are detailed in Tables 3 and 4.

Interaction: $p < 0.0001$ for each sex); *post hoc* analyses revealed that only the highest tested dose of CP55,940 (1 mg/kg i.p.) extended end expiratory pause relative to vehicle in male (1 mg/kg, $p < 0.0001$; Fig. 3E; Table 1) and female (1 mg/kg, $p < 0.0001$; Fig. 3F; Table 2) mice. End inspiratory pause was extended by CP55,940 relative to vehicle in a dose and time-dependent manner in mice of both sexes (Drug: $p < 0.0001$; Interaction: $p < 0.0001$ for each sex); CP55,940 doses 0.3 mg/kg and above extended inspiratory time in both male (0.3–1 mg/kg, $p < 0.0001$; Supplemental 1 A; Table 1) and female (0.3 mg/kg, $p = 0.0055$; 1 mg/kg, $p < 0.0001$; Supplemental 1B; Table 2) mice.

CP55,940-induced reductions in tidal volume were associated with changes to both inspiratory and expiratory effort. CP55,940 suppressed inspiratory flow relative to vehicle in a dose and time-dependent manner in mice of both sexes (Drug: $p < 0.0001$; Interaction: $p < 0.0001$ for each sex); inspiratory flow was suppressed, relative to vehicle, by all CP55,940 doses 0.1 mg/kg and higher in males (0.1–1 mg/kg; Fig. 3G; Table 1) and all CP55,940 doses 0.03 mg/kg and higher in females

Table 3
Statistical analysis of the respiratory effects of Δ^9-THC in male mice.

Metric	Time		Drug		Interaction		Effective Doses (mg/kg)				
	F	p	F	p	F	p	0.3	1	3	10	30
MV	$F_{11.352} = 169.5$	0.0001	$F_{5.32} = 23.80$	0.0001	$F_{55.352} = 13.81$	0.0001	-	-	0.0146	0.0001	0.0001
Vt	$F_{11.352} = 103.9$	0.0001	$F_{5.32} = 7.667$	0.0001	$F_{55.352} = 10.56$	0.0001	-	-	-	0.0403	0.0022
PIF	$F_{11.352} = 142.6$	0.0001	$F_{5.32} = 27.95$	0.0001	$F_{55.352} = 14.49$	0.0001	-	-	0.0008	0.0001	0.0001
PEF	$F_{11.352} = 183.5$	0.0001	$F_{5.32} = 17.14$	0.0001	$F_{55.352} = 13.93$	0.0001	-	-	-	0.0001	0.0001
Fr	$F_{11.352} = 240.0$	0.0001	$F_{5.32} = 44.90$	0.0001	$F_{55.352} = 21.85$	0.0001	-	0.0217	0.0001	0.0001	0.0001
Ti	$F_{11.352} = 147.7$	0.0001	$F_{5.32} = 49.97$	0.0001	$F_{55.352} = 23.29$	0.0001	-	-	0.0001	0.0001	0.0001
Te	$F_{11.352} = 103.1$	0.0001	$F_{5.32} = 22.72$	0.0001	$F_{55.352} = 13.13$	0.0001	-	-	0.0015	0.0001	0.0001
EIP	$F_{11.352} = 76.33$	0.0001	$F_{5.32} = 21.84$	0.0001	$F_{55.352} = 20.95$	0.0001	-	-	-	0.0001	0.0001
EEP	$F_{11.352} = 9.267$	0.0001	$F_{5.32} = 6.863$	0.0002	$F_{55.352} = 2.875$	0.0001	-	-	-	0.0019	0.0036

Data were analyzed by Two-way repeated measures ANOVA followed by Dunnett's *post hoc* test. $P < 0.05$ considered significant. Abbreviations: MV, Minute Ventilation; Vt, Tidal Volume; PIF, Peak Inspiratory Flow; PEF, Peak Expiratory Flow; Fr, Frequency; Ti, Inspiratory Time; Te, Expiratory Time; EIP, End Inspiratory Pause; EEP, End Expiratory Pause.

Table 4
Statistical analysis of the respiratory effects of Δ^9-THC in female mice.

Metric	Time		Drug		Interaction		Effective Doses (mg/kg)				
	F	p	F	p	F	p	0.3	1	3	10	30
MV	$F_{11.352} = 239.6$	0.0001	$F_{5,32} = 81.49$	0.0001	$F_{55.352} = 28.71$	0.0001	-	0.0001	0.0001	0.0001	0.0001
Vt	$F_{11.352} = 80.57$	0.0001	$F_{5,32} = 9.128$	0.0001	$F_{55.352} = 8.919$	0.0001	-	-	0.0063	0.0001	0.0001
PIF	$F_{11.352} = 152.6$	0.0001	$F_{5,32} = 92.12$	0.0001	$F_{55.352} = 22.75$	0.0001	-	0.0001	0.0001	0.0001	0.0001
PEF	$F_{11.352} = 182.0$	0.0001	$F_{5,32} = 52.68$	0.0001	$F_{55.352} = 16.95$	0.0001	-	0.0005	0.0001	0.0001	0.0001
Fr	$F_{11.352} = 152.5$	0.0001	$F_{5,32} = 14.13$	0.0001	$F_{55.352} = 12.82$	0.0001	-	-	0.0045	0.0001	0.0001
Ti	$F_{11.352} = 158.0$	0.0001	$F_{5,32} = 92.31$	0.0001	$F_{55.352} = 23.18$	0.0001	-	0.0009	0.0001	0.0001	0.0001
Te	$F_{11.352} = 148.7$	0.0001	$F_{5,32} = 41.34$	0.0001	$F_{55.352} = 20.03$	0.0001	-	-	0.0116	0.0001	0.0001
EIP	$F_{11.352} = 92.81$	0.0001	$F_{5,32} = 45.40$	0.0001	$F_{55.352} = 22.17$	0.0001	-	-	0.0010	0.0001	0.0001
EEP	$F_{11.352} = 16.07$	0.0001	$F_{5,32} = 8.021$	0.0001	$F_{55.352} = 3.897$	0.0001	-	-	-	-	0.0001

Data were analyzed by Two-way repeated measures ANOVA followed by Dunnett's *post hoc* test. $P < 0.05$ considered significant. Abbreviations: MV, Minute Ventilation; Vt, Tidal Volume; PIF, Peak Inspiratory Flow; PEF, Peak Expiratory Flow; Fr, Frequency; Ti, Inspiratory Time; Te, Expiratory Time; EIP, End Inspiratory Pause; EEP, End Expiratory Pause.

(0.03 mg/kg, $p = 0.0235$; 0.1–1 mg/kg, $p < 0.0001$; Fig. 3H; Table 2). Similarly, CP55,940 suppressed expiratory flow relative to vehicle in a dose and time dependent manner in mice of both sexes (Drug: $p < 0.0001$; Interaction: $p < 0.0001$ for each sex); expiratory flow was suppressed relative to vehicle by all CP55,940 doses 0.1 mg/kg and higher in both males (0.1–1 mg/kg, $p < 0.0001$; Supplemental 1 C; Table 1) and females (0.1–1 mg/kg, $p < 0.0001$; Supplemental 1 C; Table 2). In all analyses where dose response curves were generated, the 95 % confidence intervals for metrics impacted by CP55,940 in male and female mice overlapped, suggesting that ED_{50} values did not differ between sexes.

3.3. Respiratory effects of Δ^9-THC

Δ^9-THC markedly decreased minute ventilation relative to vehicle in a dose- and time-dependent manner in mice of both sexes (Drug: $p < 0.0001$; Interaction: $p < 0.0001$ for each sex), albeit at higher doses than observed for CP55,940. *Post hoc* comparisons revealed that all Δ^9-THC doses 3 mg/kg and above suppressed minute ventilation relative to vehicle in males (3 mg/kg, $p = 0.0146$; 10–30 mg/kg, $p < 0.0001$; Fig. 4A; Table 3), whereas all Δ^9-THC doses 1 mg/kg and above suppressed minute ventilation in females (1–30 mg/kg, $p < 0.0001$; Fig. 4B; Table 4). The ED_{50} (95 % CI) for Δ^9-THC-induced suppression of minute ventilation was 1.377 mg/kg (0.904 – 2.741) in male mice and 0.795 mg/kg (0.606 – 1.109) in female (Fig. 4C) mice.

As with CP55,940, the suppressive effect of Δ^9-THC on minute ventilation was driven by reductions to both respiratory frequency and tidal volume. Δ^9-THC reduced tidal volume relative to vehicle in a dose and time -dependent manner in mice of both sexes (Drug: $p < 0.0001$; Interaction: $p < 0.0001$; for each sex). In male mice, 10 mg/kg and 30 mg/kg doses of Δ^9-THC suppressed tidal volume relative to vehicle (10 mg/kg, $p = 0.0403$; 30 mg/kg $p = 0.0022$; Fig. 5A; Table 3) whereas doses 3 mg/kg and above suppressed tidal volume in female mice (3 mg/kg, $p = 0.0063$; 10–30 mg/kg, $p < 0.0001$; Fig. 5B; Table 4). Δ^9-THC also suppressed respiratory frequency relative to vehicle in a dose and time-dependent manner in mice of both sexes (Drug: $p < 0.0001$; Interaction: $p < 0.0001$ for each sex); Δ^9-THC doses 1 mg/kg and above suppressed respiratory frequency relative to vehicle in male mice (1 mg/kg, $p = 0.0217$; 3–30 mg/kg, $p < 0.0001$; $p < 0.0001$ vs. vehicle; Fig. 5C; Table 3), whereas Δ^9-THC doses 3 mg/kg and above suppressed respiratory frequency in female mice (3 mg/kg, $p = 0.0045$; 10–30 mg/kg, $p < 0.0001$; Fig. 5D; Table 4). The ED_{50} (95 % CI) for Δ^9-THC -induced suppression of tidal volume was 2.658 mg/kg (1.459 – 9.462) in male mice and 1.219 mg/kg (0.708 – 3.959) in female mice (Fig. 5E), whereas the ED_{50} (95 % CI) for Δ^9-THC-induced suppression of respiratory frequency was 1.397 mg/kg (0.8639–3.978) in male mice and 1.150 mg/kg (0.814 – 1.897) in female mice (Fig. 5F).

Δ^9-THC extended inspiratory time relative to vehicle in a dose and time-dependent manner in mice of both sexes (Drug: $p < 0.0001$; Interaction: $p < 0.0001$ for each sex). Inspiratory time was extended by all Δ^9-THC doses 3 mg/kg and above in male mice (3–30 mg/kg, $p < 0.0001$ vs. vehicle; Fig. 6A; Table 3) and Δ^9-THC doses 1 mg/kg and above in female mice (1 mg/kg, $p = 0.0009$; 3–30 mg/kg, $p < 0.0001$; Fig. 6B; Table 4). Δ^9-THC also extended expiratory time relative to vehicle in a dose and time-dependent manner in mice of both sexes (Drug: $p < 0.0001$; Interaction: $p < 0.0001$ for each sex). Expiratory time was increased relative to vehicle by all Δ^9-THC doses 3 mg/kg and above in both male (3 mg/kg, $p = 0.0015$; 10–30 mg/kg, $p < 0.0001$; Fig. 6C; Table 3) and female (3 mg/kg, $p = 0.0116$; 10–30 mg/kg, $p < 0.0001$; Fig. 6D; Table 4) mice. Δ^9-THC also increased the expiratory pause relative to vehicle in a dose and time-dependent manner in mice of both sexes (Male: Drug: $p = 0.0002$; Interaction: $p < 0.0001$; Female: Drug: $p < 0.0001$; Interaction: $p < 0.0001$). Expiratory pause

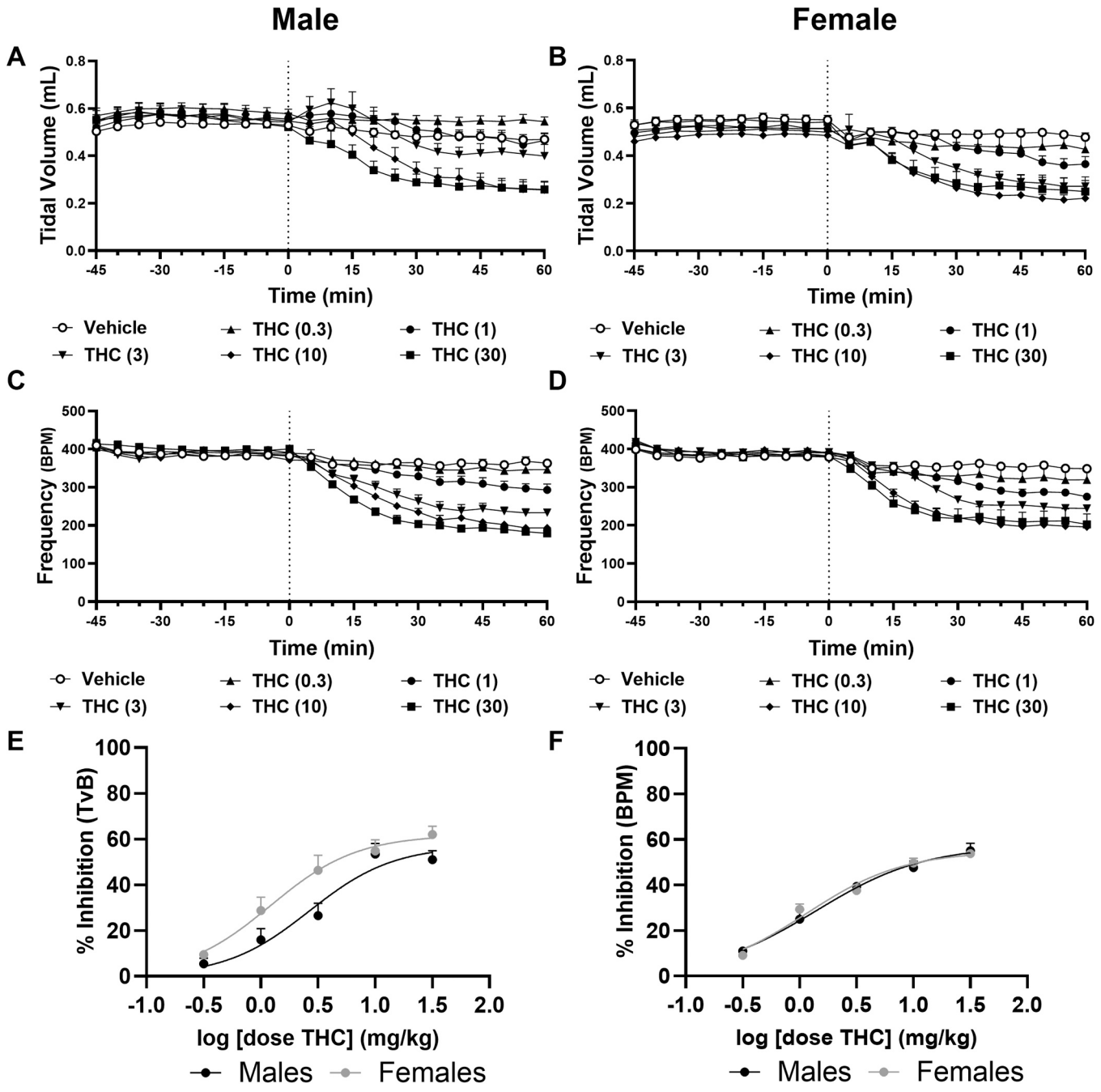

Fig. 5. Δ^9-THC reduces tidal volume and respiratory frequency in mice of both sexes. Δ^9-THC reduced tidal volume in a dose- and time-dependent manner in (**A**) male and (**B**) female mice at doses 10 mg/kg i.p. and higher in male mice and doses 3 mg/kg and higher in female mice (see Tables 3–4). THC similarly reduces respiratory frequency in both (**C**) male and (**D**) female mice. Respiratory frequency was significantly suppressed by doses 1 mg/kg and above in male mice (Tables 3) and 3 mg/kg and above in female mice (Table 4). (**E**) Dose response of Δ^9-THC in suppressing tidal volume in male and female mice. ED_{50} (95 % CI): Males: 2.658 mg/kg (1.459 – 9.462) i.p.; Females: 1.219 mg/kg (0.7077 – 3.959) mg/kg i.p. (**F**) Dose response of Δ^9-THC in suppressing respiratory frequency in male and female mice. ED_{50} (95 % CI): Males: 1.397 mg/kg (0.864 – 3.978) i.p.; Females: 1.150 mg/kg (0.814 – 1.897) i.p. (**A-D**) Data are expressed as Mean ± SEM (where visible) derived from n = 6–8 mice per group. Data were analyzed by Two-way ANOVA, Dunnett's *post hoc* test, $p < 0.05$ considered significant. All active doses $p < 0.0403$ vs. vehicle. Statistical results are detailed in Tables 3 and 4. Modest differences were detected in the pre-injection tidal volume ($p = 0.0334$) and frequency ($p = 0.0253$) in female mice. *Post hoc* tests revealed no specific differences between conditions in frequency, and persistent differences between the tidal volume of animals receiving vehicle and 10 mg/kg Δ^9-THC. No differences perseverated to the timepoint of injection.

was extended relative to vehicle by Δ^9-THC doses 10 mg/kg and above in male mice (10 mg/kg, $p = 0.0019$; 30 mg/kg, $p = 0.0036$; Fig. 6E; Table 3), but only at the highest tested dose (30 mg/kg i.p.) tested in female mice (30 mg/kg, $p < 0.0001$; Fig. 6F; Table 4). Δ^9-THC also extended the inspiratory pause relative to vehicle in a dose and time-dependent manner in mice of both sexes (Drug: $p < 0.0001$; Interaction: $p < 0.0001$ for each sex). Inspiratory pause was extended by all Δ^9-THC doses 10 mg/kg and above in male mice (10–30 mg/kg, $p < 0.0001$; Supplemental 2 A; Table 3) and all Δ^9-THC doses 3 mg/kg and above in female mice (3 mg/kg, $p = 0.0010$; 10–30 mg/kg, $p < 0.0001$; Supplemental 2B; Table 4). Δ^9-THC also reduced inspiratory flow relative to vehicle in a dose and time-dependent manner in mice of both sexes (Drug: $p < 0.0001$; Interaction: $p < 0.0001$ for each sex). Inspiratory flow was suppressed relative to vehicle by Δ^9-THC

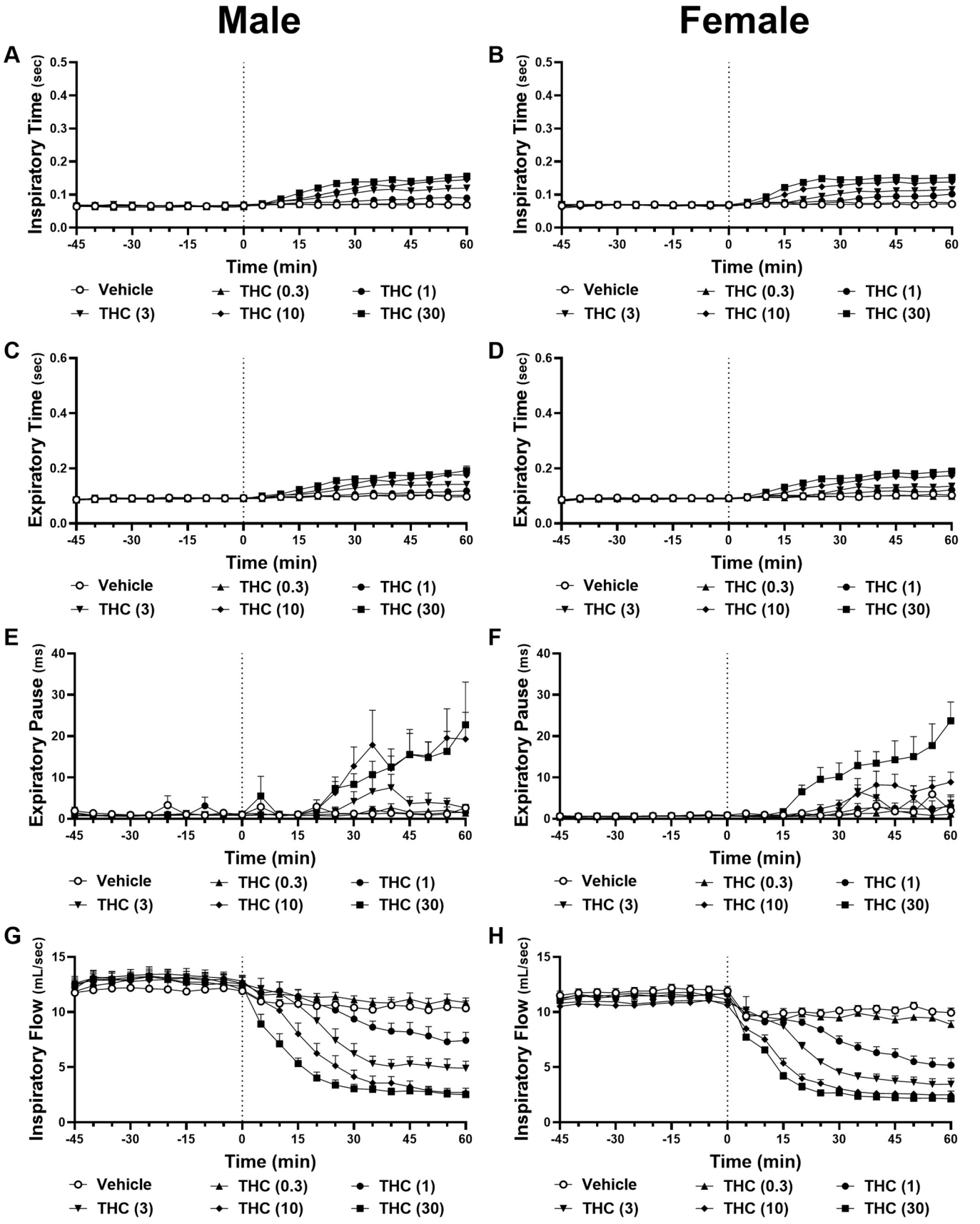

(caption on next page)

Fig. 6. Δ^9-THC prolongs inspiratory time in both (**A**) male and (**B**) female mice; doses 3 mg/kg and above increased inspiratory time in male mice, while doses 1 mg/kg and above increased inspiratory time in female mice (Tables 3 and 4). Expiratory time was similarly increased in both (**C**) male and (**D**) female mice at all doses 3 mg/kg and above in both sexes (Tables 3 and 4). Expiratory pause was extended in both (**E**) male and (**F**) female mice; 10 and 30 mg/kg i.p. doses significantly extended end expiratory pause in males (Table 3), while only the highest tested dose of 30 mg/kg extended expiratory pause in females (Table 4). Δ^9-THC reduced inspiratory flow in (**G**) male and (**H**) female mice. Inspiratory flow was suppressed by i.p. doses 3 mg/kg and above in male mice (Tables 3) and 1 mg/kg and above in female mice (Table 4). (**A-H**) Data are expressed as Mean ± SEM (where visible) derived from n = 6–8 mice per group. Data were analyzed by Two-way ANOVA, Dunnett's post hoc test, $p < 0.05$ considered significant. All active doses $p < 0.0116$ vs. vehicle. Statistical results are detailed in Tables 3 and 4. Modest but reliable baseline differences were detected in the pre-injection values of inspiratory time ($p = 0.0349$) and expiratory time ($p = 0.0245$) of female mice that subsequently received Δ^9-THC. Post hoc tests revealed no differences between the inspiratory time of specific groups, while the expiratory time of mice that subsequently received vehicle and 10 mg/kg of Δ^9-THC reliably differed. Modest but reliable baseline differences were also observed pre-injection in end inspiratory pause of groups of male mice that subsequently received administered Δ^9-THC ($p = 0.004$). *Post hoc* tests revealed modest but reliable baseline differences between mice receiving (i.p.) 1 mg/kg Δ^9-THC and mice receiving 0.3 mg/kg Δ^9-THC ($p = 0.0329$), 10 mg/kg Δ^9-THC ($p = 0.0020$), and 30 mg/kg Δ^9-THC ($p = 0.0080$). No differences between groups were observed at the time of injection.

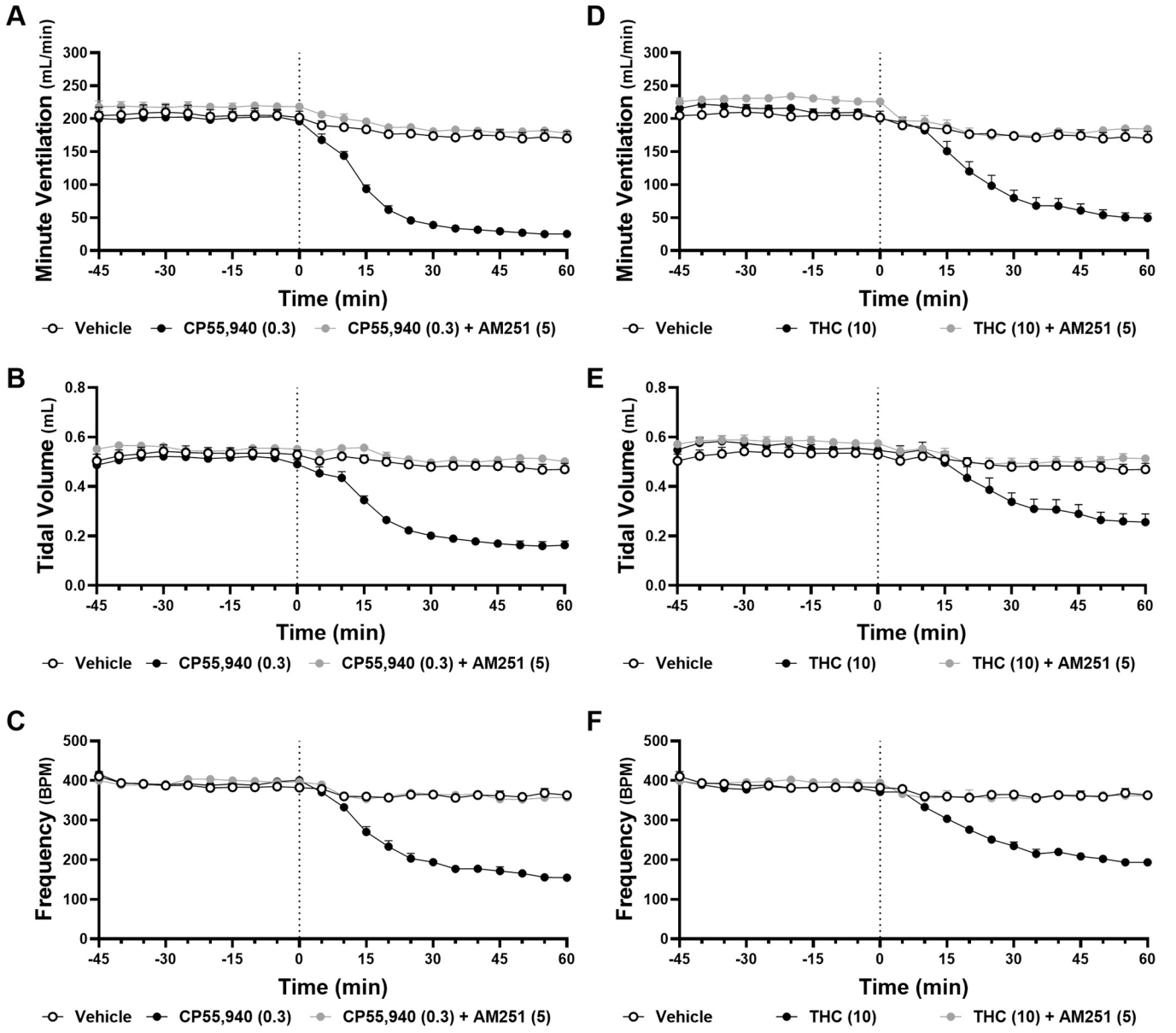

Fig. 7. The respiratory effects of CP55,94 and Δ^9-THC are mediated by CB_1 receptors. Coadministration of the centrally penetrant CB1 inverse agonist AM251 prevents CP55,940-mediated reduction of (A) minute ventilation, (B) tidal volume, and (C) respiratory frequency (Tables 5 and 6). Similarly, AM251 prevents Δ^9-THC-mediated reductions in (D) minute ventilation, (E) tidal volume, and (F) respiratory frequency (Tables 5 and 6). Respiratory metrics of mice exposed to AM251 coadministered with either CP55,940 or Δ^9-THC did not differ from vehicle controls in any tested metric. (**A-F**) Data are expressed as Mean ± SEM (where visible) derived from n = 6–8 male mice per group. Data were analyzed by Two-way ANOVA, Bonferroni's *post hoc* test, $p < 0.05$ considered significant. $p < 0.0001$ CP55,940 0.3 mg/kg vs. AM251 5 mg/kg + CP55,940 0.3 mg/kg; $p < 0.0025$ THC 10 mg/kg vs. AM251 5 mg/kg + THC 10 mg/kg. Statistical results are detailed in Tables 5 and 6.

Table 5
Statistical analysis of the effects of AM251 on CP55,940-induced respiratory suppression in male mice.

Metric	Time		Drug		Interaction		vs. CP55,940	vs. Vehicle
	F	p	F	p	F	p		
MV	$F_{11,187} = 91.99$	0.0001	$F_{2,17} = 37.03$	0.0001	$F_{22,187} = 37.03$	0.0001	0.0001	-
Vt	$F_{11,187} = 78.45$	0.0001	$F_{2,17} = 99.65$	0.0001	$F_{22,187} = 31.84$	0.0001	0.0001	-
PIF	$F_{11,187} = 48.45$	0.0001	$F_{2,17} = 153.6$	0.0001	$F_{22,187} = 22.07$	0.0001	0.0001	-
PEF	$F_{11,187} = 73.08$	0.0001	$F_{2,17} = 147.0$	0.0001	$F_{22,187} = 28.17$	0.0001	0.0001	-
Fr	$F_{11,187} = 75.52$	0.0001	$F_{2,17} = 127.2$	0.0001	$F_{22,187} = 51.41$	0.0001	0.0001	-
Ti	$F_{11,187} = 52.91$	0.0001	$F_{2,17} = 154.5$	0.0001	$F_{22,187} = 50.51$	0.0001	0.0001	-
Te	$F_{11,187} = 43.52$	0.0001	$F_{2,17} = 72.55$	0.0001	$F_{22,187} = 33.44$	0.0001	0.0001	-
EIP	$F_{11,187} = 37.18$	0.0001	$F_{2,17} = 68.03$	0.0001	$F_{22,187} = 34.43$	0.0001	0.0001	-
EEP	$F_{11,187} = 9.497$	0.0001	$F_{2,17} = 35.45$	0.0001	$F_{22,187} = 8.598$	0.0001	0.0001	-

Data were analyzed by Two-way repeated measures ANOVA followed by Bonferroni *post hoc* test. $P < 0.05$ considered significant. Abbreviations: MV, Minute Ventilation; Vt, Tidal Volume; PIF, Peak Inspiratory Flow; PEF, Peak Expiratory Flow; Fr, Frequency; Ti, Inspiratory Time; Te, Expiratory Time; EIP, End Inspiratory Pause; EEP, End Expiratory Pause.

Table 6
Statistical analysis of the effects of AM251 on Δ^9-THC-induced respiratory suppression in male mice.

Metric	Time		Drug		Interaction		vs. THC	vs. Vehicle
	F	p	F	p	F	p		
MV	$F_{11,187} = 78.68$	0.0001	$F_{2,17} = 78.68$	0.0001	$F_{22,187} = 78.68$	0.0001	0.0001	-
Vt	$F_{11,187} = 73.32$	0.0001	$F_{2,17} = 9.713$	0.0015	$F_{22,187} = 32.28$	0.0001	0.0025	-
PIF	$F_{11,187} = 48.20$	0.0001	$F_{2,17} = 41.24$	0.0001	$F_{22,187} = 28.99$	0.0001	0.0001	-
PEF	$F_{11,187} = 62.23$	0.0001	$F_{2,17} = 25.31$	0.0001	$F_{22,187} = 30.34$	0.0001	0.0001	-
Fr	$F_{11,187} = 45.31$	0.0001	$F_{2,17} = 65.22$	0.0001	$F_{22,187} = 37.63$	0.0001	0.0001	-
Ti	$F_{11,187} = 54.56$	0.0001	$F_{2,17} = 138.0$	0.0001	$F_{22,187} = 51.85$	0.0001	0.0001	-
Te	$F_{11,187} = 24.85$	0.0001	$F_{2,17} = 35.45$	0.0001	$F_{22,187} = 23.74$	0.0001	0.0001	-
EIP	$F_{11,187} = 37.15$	0.0001	$F_{2,17} = 42.01$	0.0001	$F_{22,187} = 35.89$	0.0001	0.0001	-
EEP	$F_{11,187} = 2.761$	0.0024	$F_{2,17} = 7.145$	0.0056	$F_{22,187} = 4.550$	0.001	0.0386	-

Data were analyzed by Two-way repeated measures ANOVA followed by Bonferroni *post hoc* test. $P < 0.05$ considered significant. Abbreviations: MV, Minute Ventilation; Vt, Tidal Volume; PIF, Peak Inspiratory Flow; PEF, Peak Expiratory Flow; Fr, Frequency; Ti, Inspiratory Time; Te, Expiratory Time; EIP, End Inspiratory Pause; EEP, End Expiratory Pause.

doses 3 mg/kg and above in male mice (3 mg/kg, $p = 0.0008$; 10–30 mg/kg, $p < 0.0001$; Fig. 6G; Tables 3), and 1 mg/kg and above in female mice (1–30 mg/kg, $p < 0.0001$; Fig. 6H; Table 4). Δ^9-THC also reduced expiratory flow relative to vehicle in a dose and time-dependent manner in mice of both sexes (Drug: $p < 0.0001$; Interaction: $p < 0.0001$ for each sex). Expiratory flow was suppressed relative to vehicle by Δ^9-THC doses 10 mg/kg and above in male mice (10 mg/kg, $p = 0.0001$; 30 mg/kg, $p < 0.0001$; Supplemental 2 C; Table 3) and 1 mg/kg and above in female mice (1 mg/kg, $p = 0.0005$; 3–30 mg/kg, $p < 0.0001$; Supplemental 2D; Table 4). In all analyses where dose response curves were generated, the 95 % confidence intervals for metrics impacted by Δ^9-THC in male and female mice overlapped, suggesting that ED_{50} values did not differ between sexes.

3.4. Respiratory effects of CB_1 agonists are reversed by the global CB_1 antagonist AM251 and partially attenuated by the peripherally restricted CB_1 antagonist AM6545

Coadministration of AM251 (5 mg/kg i.p.) with CP55,940 (0.3 mg/kg i.p.) blocked the respiratory suppressive effects of CP55,940 (0.3 mg/kg i.p.). Coadministration of AM251 (5 mg/kg i.p.) blocked the respiratory suppressive effects of CP55,940 (0.3 mg/kg i.p.) (Drug: $p < 0.0001$; Interaction: $p < 0.0001$ for each metric) on minute ventilation ($p < 0.0001$; Fig. 7A; Table 5), tidal volume ($p < 0.0001$; Fig. 7B; Table 5), and respiratory frequency ($p < 0.0001$; Fig. 7C; Table 5). Coadministration of AM251 (5 mg/kg i.p.) similarly blocked (Drug: $p < 0.0016$; Interaction: $p < 0.0001$ for each metric) the respiratory suppressive effects of Δ^9-THC (10 mg/kg i.p.) on minute ventilation ($p < 0.0001$; Fig. 7D; Table 6), tidal volume ($p = 0.0025$; Fig. 7E; Table 6), and respiratory frequency ($p < 0.0001$; Fig. 7F; Table 6). Coadministration of AM251 (5 mg/kg i.p.) also blocked (Drug: $p < 0.0001$; Interaction: $p < 0.0001$ for all metrics) CP55,940 (0.3 mg/kg i.p.)-induced extensions of inspiratory time ($p < 0.0001$; Fig. 8A; Table 5), expiratory time ($p < 0.0001$; Fig. 8B; Table 5), expiratory pause ($p < 0.0001$; Fig. 8C; Table 5), and reductions of inspiratory flow ($p < 0.0001$; Fig. 8D; Table 5). Furthermore, coadministration of AM251 (5 mg/kg i.p.) also blocked (Drug: $p < 0.0001$; Interaction: $p < 0.0001$ for each metric) Δ^9-THC (10 mg/kg i.p.)-induced extensions of inspiratory time ($p < 0.0001$; Fig. 8E; Table 6) and expiratory time ($p < 0.0001$; Fig. 8F; Table 6). AM251 (5 mg/kg i.p.) coadministration also blocked (Drug: $p = 0.0056$; Interaction: $p = 0.0001$) Δ^9-THC-induced extensions of the expiratory pause ($p = 0.0386$; Fig. 8G; Table 6), and reductions (Drug: $p < 0.0001$; Interaction: $p < 0.0001$) of inspiratory flow ($p < 0.0001$; Fig. 8H; Table 6). Coadministration of AM251 additionally blocked (Drug: $p < 0.0001$; Interaction: $p < 0.0001$ for each agonist) reductions to expiratory flow induced by CP55,940 ($p < 0.0001$; Supplemental 4 A; Table 5) and Δ^9-THC ($p < 0.0001$; Supplemental 4B; Table 6), as well as elongations (Drug: $p < 0.0001$; Interaction: $p < 0.0001$ for each agonist) to inspiratory pause induced by CP55,940 ($p < 0.0001$; Supplemental 4 C; Table 5) and Δ^9-THC ($p < 0.0001$; Supplemental 4D; Table 6).

In contrast, the peripherally restricted CB_1 antagonist AM6545 (10 mg/kg i.p.) modestly but reliably lessened the respiratory suppressive effects produced by CP55,940 (0.3 mg/kg i.p.) (Drug: $p < 0.0001$; Interaction: $p < 0.0001$ for each metric) on minute ventilation ($p = 0.0044$; Table 7; Fig. 9A), tidal volume ($p = 0.0040$; Table 7; Fig. 9B), and respiratory frequency ($p = 0.0406$; Table 7; Fig. 9C).

The respiratory suppressive effects of Δ^9-THC (10 mg/kg i.p.) (Drug: $p < 0.0013$; Interaction: $p < 0.0001$ for each metric) on minute ventilation (Table 8; Fig. 9D), tidal volume (Table 8; Fig. 9E), and respiratory frequency (Table 8; Fig. 9F) were not blocked by coadministration of AM6545 (10 mg/kg i.p.) ($p > 0.9999$ vs. Δ^9-THC 10 mg/kg for each metric).

AM6545 (10 mg/kg) partially blocked (Drug: $p < 0.0001$;

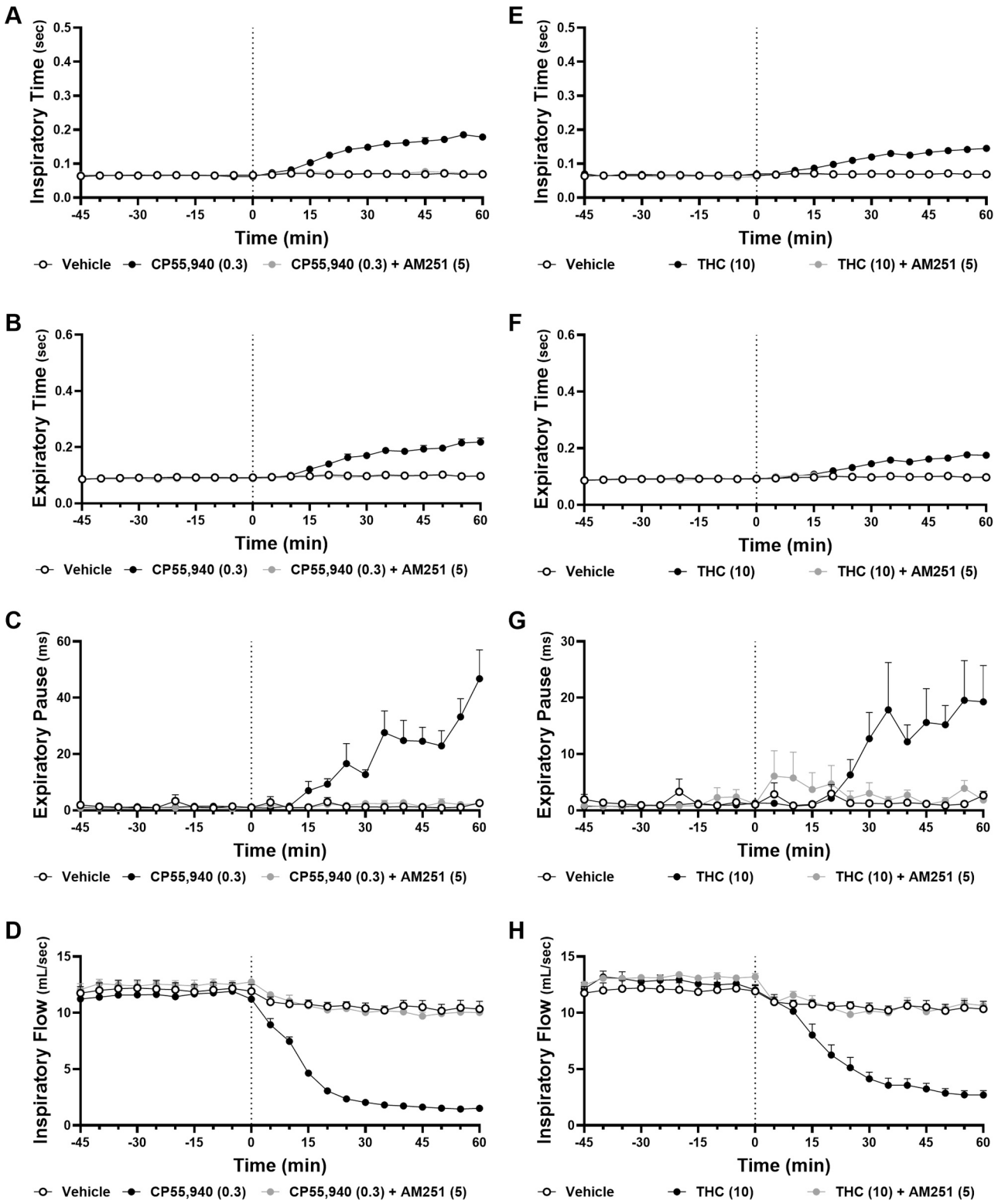

Fig. 8. The centrally penetrant CB_1 antagonist AM251 prevents the respiratory effects of both CP55,940 and Δ^9-THC across all tested metrics. Coadministration of AM251 prevents CP55,940-induced elongation of **(A)** inspiratory time, **(B)** expiratory time, and **(C)** expiratory pause, while preventing reductions of **(D)** inspiratory flow. AM251 similarly prevented Δ^9-THC-induced elongation of **(E)** inspiratory time, **(F)** expiratory time, and **(G)** expiratory pause, while preventing reductions of **(H)** inspiratory flow. Effects of AM251 and CP55,940 coadministration doses did not differ from vehicle controls in any tested metric. **(A-H)** Data are expressed as Mean ± SEM (where visible) derived from n = 6–8 male mice per group. Data were analyzed by Two-way ANOVA, Bonferroni's *post hoc* test, $p < 0.05$ considered significant. $p < 0.0001$ CP55,940 0.3 mg/kg vs. AM251 5 mg/kg + CP55,940 0.3 mg/kg; $p < 0.0386$ THC 10 mg/kg vs. AM251 5 mg/kg + THC 10 mg/kg. Statistical results are detailed in Tables 5 and 6. Modest but reliable differences in end expiratory pause were detected in the pre-injection baselines of mice injected subsequently with vehicle and 10 mg/kg Δ^9-THC ($p = 0.0045$). These differences were not observed at the time of injection.

Table 7
Statistical analysis of the effects of AM6545 on CP55,940-induced respiratory suppression in male mice.

Metric	Time		Drug		Interaction		vs. CP55,940	vs. Vehicle
	F	p	F	p	F	p		
MV	$F_{11,176} = 154.8$	0.0001	$F_{2,16} = 109.2$	0.0001	$F_{22,176} = 31.69$	0.0001	0.0044	0.0001
Vt	$F_{11,176} = 93.71$	0.0001	$F_{2,16} = 37.75$	0.0001	$F_{22,176} = 21.77$	0.0001	0.0040	0.0008
PIF	$F_{11,176} = 117.2$	0.0001	$F_{2,16} = 128.4$	0.0001	$F_{22,176} = 33.95$	0.0001	0.0092	0.0001
PEF	$F_{11,176} = 124.4$	0.0001	$F_{2,16} = 68.76$	0.0001	$F_{22,176} = 24.38$	0.0001	0.0052	0.0001
Fr	$F_{11,176} = 96.08$	0.0001	$F_{2,16} = 93.62$	0.0001	$F_{22,176} = 23.89$	0.0001	0.0406	0.0001
Ti	$F_{11,176} = 46.52$	0.0001	$F_{2,16} = 35.59$	0.0001	$F_{22,176} = 18.14$	0.0001	0.0127	0.0001
Te	$F_{11,176} = 21.71$	0.0001	$F_{2,16} = 13.67$	0.0003	$F_{22,176} = 7.027$	0.0001	-	0.0412
EIP	$F_{11,176} = 45.49$	0.0001	$F_{2,16} = 34.08$	0.0001	$F_{22,176} = 18.71$	0.0001	0.0016	0.0001
EEP	$F_{11,176} = 3.145$	0.0007	$F_{2,16} = 2.331$	0.1293	$F_{22,176} = 2.206$	0.0025	-	-

Data were analyzed by Two-way repeated measures ANOVA followed by Bonferroni *post hoc* test. $P < 0.05$ considered significant. Abbreviations: MV, Minute Ventilation; Vt, Tidal Volume; PIF, Peak Inspiratory Flow; PEF, Peak Expiratory Flow; Fr, Frequency; Ti, Inspiratory Time; Te, Expiratory Time; EIP, End Inspiratory Pause; EEP, End Expiratory Pause.

Interaction: $p < 0.0001$ for each metric) CP55,940 (0.3 mg/kg)-induced extensions of inspiratory time ($p = 0.0127$ vs. CP55,940; $p = 0.0005$ vs. vehicle; Fig. 10A; Table 7) and reductions of inspiratory flow ($p = 0.0092$ vs. CP55,940; $p < 0.0001$ vs. vehicle; Fig. 10B; Table 7). CP55,940 (0.3 mg/kg)-induced extensions of expiratory time (Drug: $p = 0.0003$; Interaction: $p < 0.0001$; $p = 0.0946$ vs. CP55,940; Fig. 10C; Table 7) and expiratory pause (Drug: $p = 0.1293$; Interaction: $p = 0.0025$; $p = 0.1847$ vs. CP55,940; Fig. 10D; Table 7) in the AM6545 coadministration group did not differ from that observed in mice exposed to CP55,940 alone. AM6545 (10 mg/kg i.p.) failed to block Δ^9-THC (10 mg/kg i.p)-induced (Drug: $p < 0.0001$; Interaction $p < 0.0001$ for each metric) extensions of inspiratory time ($p = 0.7126$ vs. Δ^9-THC; Fig. 10E; Table 8), reductions of inspiratory flow ($p > 0.9999$ vs. Δ^9-THC; Fig. 10F; Table 8), or extension of expiratory time ($p > 0.9999$ vs. Δ^9-THC; Fig. 10G; Table 8). However, THC-induced elevations in expiratory pause were completely blocked (Drug: $p = 0.0014$; Interaction: $p < 0.0001$; $p = 0.0041$ vs. Δ^9-THC; $p > 0.9999$ vs. vehicle; Fig. 10H; Table 8) by coadministration of AM6545.

Coadministration with AM6545 partially blocked reductions (Drug: $p < 0.0001$; Interaction: $p < 0.0001$ for each agonist) to expiratory flow induced by CP55.940 ($p = 0.0052$ vs. CP55,940; $p < 0.0001$ vs. vehicle; Supplemental 4E; Table 7) but did not alter the effects of Δ^9-THC ($p > 0.9999$ vs. Δ^9-THC 10 mg/kg; $p < 0.0001$ vs. vehicle; Supplemental 4 F; Table 8).

AM6545 did not completely prevent the respiratory suppressive effects of CP55,940; all metrics impacted by the tested dose of CP55,940 remained suppressed in comparison to vehicle controls (Fig. 9A-C; Fig. 10A-D; Supplemental 4G-H; Table 7). Doses of AM251 and AM6545 used in coadministration experiments had no intrinsic effects on respiratory activity when administered alone (Supplemental 3A-I).

3.5. CB_1 mRNA is expressed in the pre-Bötzinger complex

The general consensus on the relative safety of cannabis compared to opioids is largely based on the very low levels of CB_1 receptors in the medulla determined by autoradiography [2,33]. To determine whether mRNA for CB_1 receptors is expressed by respiratory neurons, we employed RNAScope *in situ* hybridization, a technique that offers superior detection sensitivity. The pre-Bötzinger complex was readily visualized by the high concentration of *Oprm1*-expressing cells, in agreement with the well-established respiratory effect of μ-opioid receptor (MOR) activation (Fig. 11A). Respiratory neurons in the pre--Bötzinger complex were labeled by the presence of *Tacr1* mRNA, encoding the Neurokinin 1 receptor, a marker of these cells. Importantly, we found *Cnr1* mRNA (encoding the CB_1 receptor) in 27 % of all pre-Bötzinger cells and in approximately 33 % of all respiratory cells (expressing *Tacr1* mRNA) in wild-type mice. In contrast, only 4 % of pre-Bötzinger complex cells contained an RNAscope signal in sections obtained from $CB_1^{-/-}$ mice (Fig. 11D-F). Extensive colocalization of *Cnr1*- and *Oprm1*-expressing cells was observed (Fig. 11B). On average, 87 % of *Cnr1*-expressing cells also expressed *Oprm1*, a population that made up 33 % of all cells expressing *Oprm1*. Triple-labeled *Cnr1-Tacr1-Oprm1*-expressing cells (Fig. 11B) made up 87 % of *Cnr1*-labeled respiratory cells and 36 % of Oprm1-labeled respiratory cells. These data, taken together, indicate that about one third of respiratory neurons express *Cnr1* in the respiratory center of the medulla and that CB_1 receptors are extensively colocalized in *Oprm1*-expressing respiratory cells known to contribute to opioid overdose.

4. Discussion

Little is currently known about how CB_1 activation affects respiratory function. Only low levels of cannabinoid receptor binding are detected in the medulla, ostensibly explaining why high doses of cannabis are rarely lethal [2]. However, users of illicit synthetic cannabinoids suffer from a variety of life-threatening side effects, including cardiovascular complications and acute respiratory depression [8–13]. Synthetic cannabinoid use and overdose rates are poorly tracked and complicated by unstable pharmacology, a lack of consistent testing, and the absence of standardized, commercially available tests. Nonetheless, synthetic cannabinoids remain the most widely used class of new psychoactive compounds in the United States, and coadministration of synthetic cannabinoids and opioids has recently been documented in lethal overdose [14,15,34,35]. No antidote is available for synthetic cannabinoid overdose, and treatment is limited to supportive care [9]. Attempts to treat cannabinoid-induced respiratory depression with existing reversal agents (e.g., naloxone) have met with generally negative results [36–38]. Our studies suggest that the existence of detrimental respiratory effects of CB_1 agonists must be recognized.

Using whole body plethysmography, we showed that the synthetic bicyclic cannabinoid CP55,940 and the phytocannabinoid Δ^9-THC produce respiratory depression in awake mice in a CB_1-dependent manner. Changes were rapid, dose-dependent, and persistent. Both cannabinoids impacted each phase of the respiratory cycle by reducing inspiratory and expiratory flow and extending inspiratory and expiratory time. These effects translated into severe depression of respiratory frequency, tidal volume, and minute ventilation that persisted for over one hour. All respiratory parameters were impacted by at least one tested dose of CP55,940 and Δ^9-THC, but the doses at which these effects occurred were not uniform. Parameters that assess the characteristics of individual breaths (i.e., flow rate and phase time) were inhibited before parameters that measure the time between respiratory phases (i.e., inspiratory and expiratory pause). Thus, changes to respiratory frequency and overall respiratory activity were primarily mediated by changes to the characteristics of individual breaths rather than by changes to the interval between them.

The suppressive effects of Δ^9-THC on respiratory activity are striking given its widespread use and the sparse nature of human overdoses. A

floor effect was observed in Δ^9-THC's effect on minute ventilation in mice of both sexes (~50 mL/minute in males and ~45 mL/minute in females); the 10 mg/kg and 30 mg/kg dose reduced minute ventilation to similar levels. Thus, the lack of Δ^9-THC overdoses observed in humans may be attributable to partial agonism-induced limitations in drug efficacy that limit respiratory effects to levels that do not constitute a clinical emergency. Consistent with this hypothesis, no dose of Δ^9-THC recapitulated levels of respiratory suppression seen with CP55,940, in which near-total elimination of respiratory activity was observed at the highest tested doses. Despite the magnitude of respiratory suppression observed in experiments utilizing synthetic CB_1 receptor agonists, we did not observe overdose deaths from cannabinoids in any of our studies.

The respiratory effects of CP55,940 and Δ^9-THC were mediated by CB_1 receptors. The CNS-penetrant CB_1 inverse agonist AM251 completely reversed the effects of both CP55,940 and Δ^9-THC, indicating that observed effects were entirely mediated by activity at the CB_1 receptor. The peripherally-restricted CB_1 antagonist AM6545 partially, but reliably, attenuated the respiratory effects of CP55,940, and some of the respiratory effects of Δ^9-THC. Thus, cannabinoid-induced respiratory effects are primarily mediated by CB_1 receptors in the CNS with modest contribution from peripheral CB_1 receptors under some circumstances. Two notable exceptions to this pattern were observed.

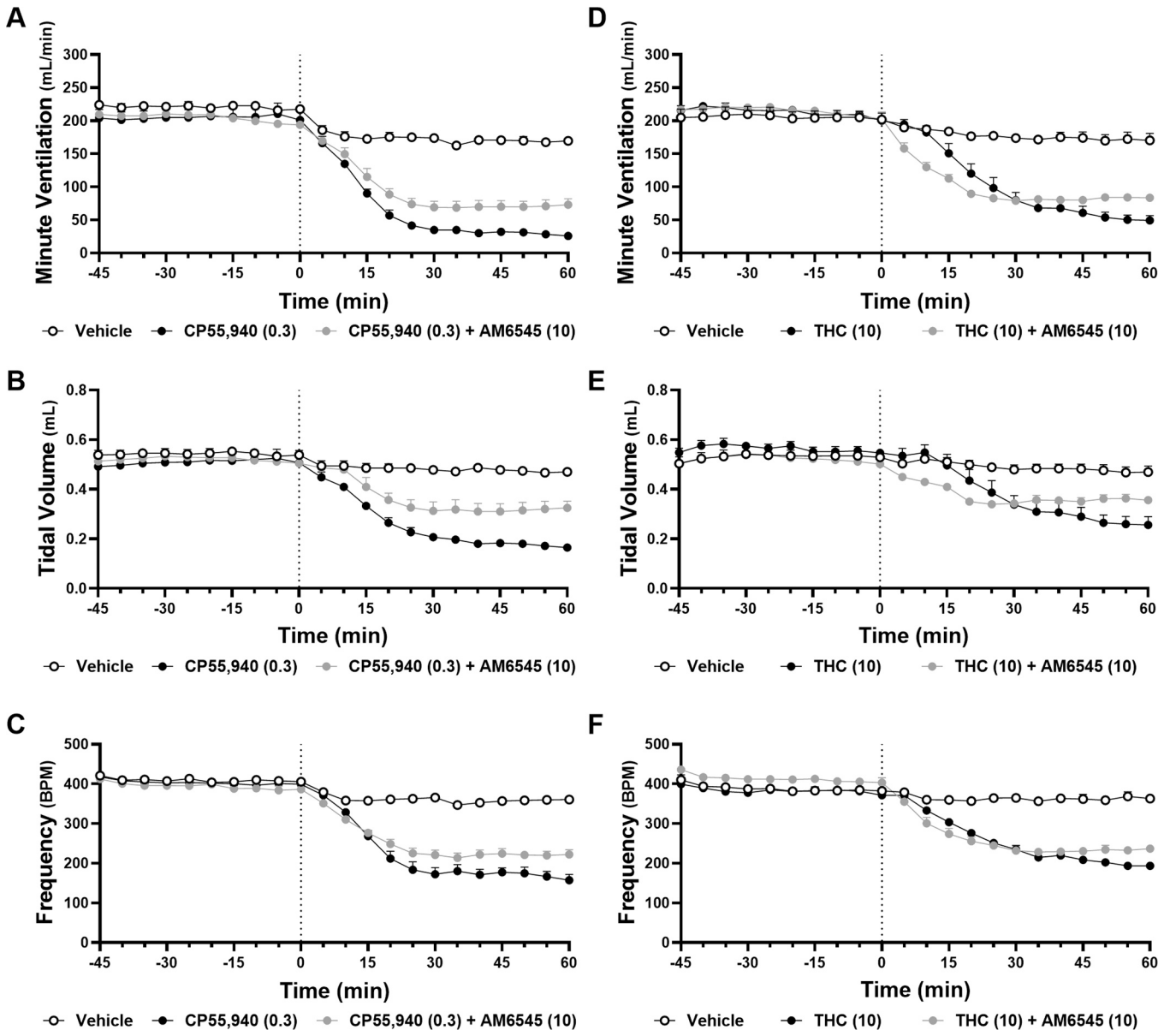

Fig. 9. The peripherally restricted CB_1 antagonist AM6545 partially and inconsistently prevented the respiratory effects of CP55,940 and Δ^9-THC. The peripherally restricted CB_1 antagonist AM6545 attenuated but did not prevent the respiratory effects of CP55,940 across most metrics. (**A**) Minute ventilation (**B**) tidal volume, and (**C**) respiratory frequency of mice exposed to both CP55,940 and AM6545 differed from those receiving only CP55,940 although metrics failed to normalize to vehicle controls in all instances (Table 7). In contrast, the (**D**) minute ventilation, (**E**) tidal volume, and (**F**) frequency of animals exposed to both Δ^9-THC and AM6545 did not differ from animals exposed only to Δ^9-THC (Table 8). Modest but reliable baseline differences were observed in pre-injection respiratory frequency ($p = 0.0062$). *Post hoc* analysis revealed modest baseline differences between the frequency of the vehicle and Δ^9-THC 10 mg/kg groups ($p = 0.0198$), the frequency Δ^9-THC 10 mg/kg and Δ^9-THC 10 mg/kg + AM6545 10 mg/kg groups ($p = 0.0105$). No differences between groups were observed at the time of injection. Data are expressed as Mean ± SEM (where visible) derived from $n = 6$ male mice per group. Data were analyzed by Two-way ANOVA, Bonferroni's *post hoc* test, $p < 0.05$ considered significant. $p < 0.0406$ for significant reversal of CP55,940 0.3 mg/kg vs. AM6545 10 mg/kg + CP55,940 0.3 mg/kg; no significant reversal of THC 10 mg/kg vs. AM6545 10 mg/kg + THC 10 mg/kg. Statistical results are detailed in Tables 7 and 8.

Table 8
Statistical analysis of the effects of AM6545 on Δ^9-THC-induced respiratory suppression in male mice.

Metric	Time		Drug		Interaction		vs. THC	vs. Vehicle
	F	p	F	p	F	p		
MV	$F_{11,187} = 139.5$	0.0001	$F_{2,17} = 43.30$	0.0001	$F_{22,187} = 36.07$	0.0001	-	0.0001
Vt	$F_{11,187} = 68.36$	0.0001	$F_{2,17} = 10.33$	0.0012	$F_{22,187} = 22.69$	0.0001	-	0.0044
PIF	$F_{11,187} = 87.59$	0.0001	$F_{2,17} = 56.49$	0.0001	$F_{22,187} = 29.69$	0.0001	-	0.0001
PEF	$F_{11,187} = 102.5$	0.0001	$F_{2,17} = 32.73$	0.0001	$F_{22,187} = 29.37$	0.0001	-	0.0001
Fr	$F_{11,187} = 105.5$	0.0001	$F_{2,17} = 71.42$	0.0001	$F_{22,187} = 29.73$	0.0001	-	0.0001
Ti	$F_{11,187} = 95.45$	0.0001	$F_{2,17} = 67.66$	0.0001	$F_{22,187} = 40.07$	0.0001	-	0.0001
Te	$F_{11,187} = 59.49$	0.0001	$F_{2,17} = 30.12$	0.0001	$F_{22,187} = 18.49$	0.0001	-	0.0001
EIP	$F_{11,187} = 48.86$	0.0001	$F_{2,17} = 30.40$	0.0001	$F_{22,187} = 27.63$	0.0001	0.0022	0.0103
EEP	$F_{11,187} = 5.631$	0.0001	$F_{2,17} = 9.983$	0.0014	$F_{22,187} = 4.650$	0.0001	0.0041	-

Data were analyzed by Two-way repeated measures ANOVA followed by Bonferroni *post hoc* test. $P < 0.05$ considered significant. Abbreviations: MV, Minute Ventilation; Vt, Tidal Volume; PIF, Peak Inspiratory Flow; PEF, Peak Expiratory Flow; Fr, Frequency); Ti, Inspiratory Time; Te, Expiratory Time; EIP, End Inspiratory Pause; EEP, End Expiratory Pause

AM6545 completely prevented the Δ^9-THC-induced extension of expiratory pause, and completely and partially prevented the extension of the inspiratory pause induced by CP55,940 and Δ^9-THC, respectively. Thus, peripheral CB_1 receptors may play a role in maintaining the transition between inspiration and expiration. CB_1 receptors are sparsely expressed in carotid body chemoreceptors, peripheral components of the respiratory system that modulate respiratory activity by sensing the partial pressure of oxygen and carbon dioxide in blood entering the brain through the carotid artery [39,40] and thus may represent a potential site of action for respiratory control of peripheral CB_1 receptors. In the presence of AM6545, suppressive effects of Δ^9-THC on peak inspiratory and expiratory flow occurred earlier, suggesting that blocking peripheral CB_1 receptors exacerbated the effects of Δ^9-THC on inspiratory and expiratory flow.

Respiratory effects of cannabinoids were observed at doses commonly used for behavioral testing, and often at doses lower than those that produce cardinal behavioral signs of CB_1 activation: hypothermia, catalepsy, analgesia, and locomotor suppression [41]. Behaviors measured in the classical cannabinoid tetrad [42] could be impacted by respiratory suppression (e.g., open field or ring test). A mouse respirating at a small fraction of its normal rate can be expected to show lower than normal levels of locomotion. Additionally, changes to tidal volume in opioid-induced respiratory depression are partially attributable to changes in chest muscle rigidity [1,43,44]. Hence, chest muscle rigidity produced by cannabinoid agonists could potentially contribute to the changes in tidal volume observed here. Hypothermia has similarly been shown to suppress respiratory activity [45], further suggesting a reciprocal relationship between the behavioral and respiratory effects of cannabinoid agonists.

Opioids primarily depress respiration in awake animals by eliciting changes in respiratory frequency; changes to tidal volume are observed inconsistently, and typically only at high doses or with high-potency synthetic agonists [46,47]. CB_1 agonists profoundly reduced all tested respiratory parameters and, consequently, only partially recapitulated this pattern. CP55,940 generally produced respiratory suppressive effects at similar doses in both male and female mice, whereas Δ^9-THC generally produced respiratory suppressive effects at lower doses in females than males. To our knowledge, sex differences in cannabinoid overdose are unexplored in the current literature. Δ^9-THC and its active metabolites have been shown to exhibit increased potency in female animals in various models, while the metabolites of CP55,940 remain largely unexplored [48]. The topic of sex differences in overdose is an emerging one, and more work is necessary to determine whether possible differences in responsiveness to chronic dosing between sexes could be attributed to differential metabolism of these drugs in males and females, differences in CYP metabolism or induction, or differences in CB_1 receptor density or efficacy in relevant brain regions. The overlap of the 95 % confidence intervals on all dose response curves nonetheless showed the ED_{50} was similar between sexes for each agonist, administered acutely.

References to the absence of CB_1 in respiratory control nuclei and to cannabinoids lacking deleterious respiratory effects abound in current literature and have supported the view that cannabinoids are superior alternatives to opioid-based analgesics on the basis that they lack respiratory complications [2,49]. However, our studies and others suggest that these conventions are not supported by data. Our histological results support the hypothesis that CB_1-induced respiratory depression may involve neural substrates that overlap with those of opioids. Using RNAscope *in situ* hybridization, we demonstrate the presence of *Cnr1* mRNA-expressing cells in the pre-Bötzinger complex. The RNAscope signal representing *Cnr1* mRNA was largely absent in $CB_1^{-/-}$ mice, verifying the specificity of the probe. Furthermore, we found that the vast majority (87 %) of *Cnr1* mRNA-expressing respiratory cells co-expressed *Oprm1* mRNA (Table 9). Conversely, a subpopulation of *Oprm1* mRNA-expressing cells (33 %) or *Tacr1*-expressing cells (33 %) co-expressed *Cnr1* mRNA. Thus, CB_1-induced depression of respiratory rate may be mediated, at least in part, by CB_1-expressing cells in the pre-Bötzinger complex.

We did not directly assess sites of action because our studies employed systemic injections. Nonetheless, CB_1 expression in the pre-Bötzinger complex represents a possible site of action for the respiratory effects of CB_1 agonists observed in our experiments. However, expression in the pre-Bötzinger complex is unlikely to drive changes in tidal volume and other respiratory metrics impacted by CB_1 agonists in our experiments that are not attributable to changes in inspiratory rhythm generation, suggesting the existence of additional sites of action. Further work is required to establish the precise distribution and contribution of CB_1-expressing cells in the pre-Bötzinger complex and other brain regions responsible for respiratory control, such as the parabrachial nucleus, parafacial nucleus, nucleus tractus solitarius and Kölliker-Fuse nucleus [50–53].

Few brain regions directly implicated in respiratory control have been specifically characterized for CB_1 expression, and the expression of CB_1 receptors in respiratory neurons has not previously been evaluated. CB_1 mRNA has been confirmed in the C1 and A1 regions of the RVLM of the rat by qPCR [54], but these experiments were not coupled with direct measures of respiratory activity. CB_1 mRNA expression has been reported using qPCR in the pre-Bötzinger complex [22], but both the RVLM and pre-Bötzinger complex contain populations of respiratory and non-respiratory neurons. Thus, these approaches do not address the anatomical distribution of receptors within these brain regions or phenotypes of CB_1-expressing neurons. More work is necessary to confirm the presence of neurons expressing CB_1 protein in the pre-Bötzinger complex and other brainstem respiratory regions, and to establish the contribution of CB_1 receptors in respiratory regions to the control of breathing.

Taken together, our findings demonstrate that both phytocannabinoid and synthetic CB_1 agonists induce respiratory depression in a dose-

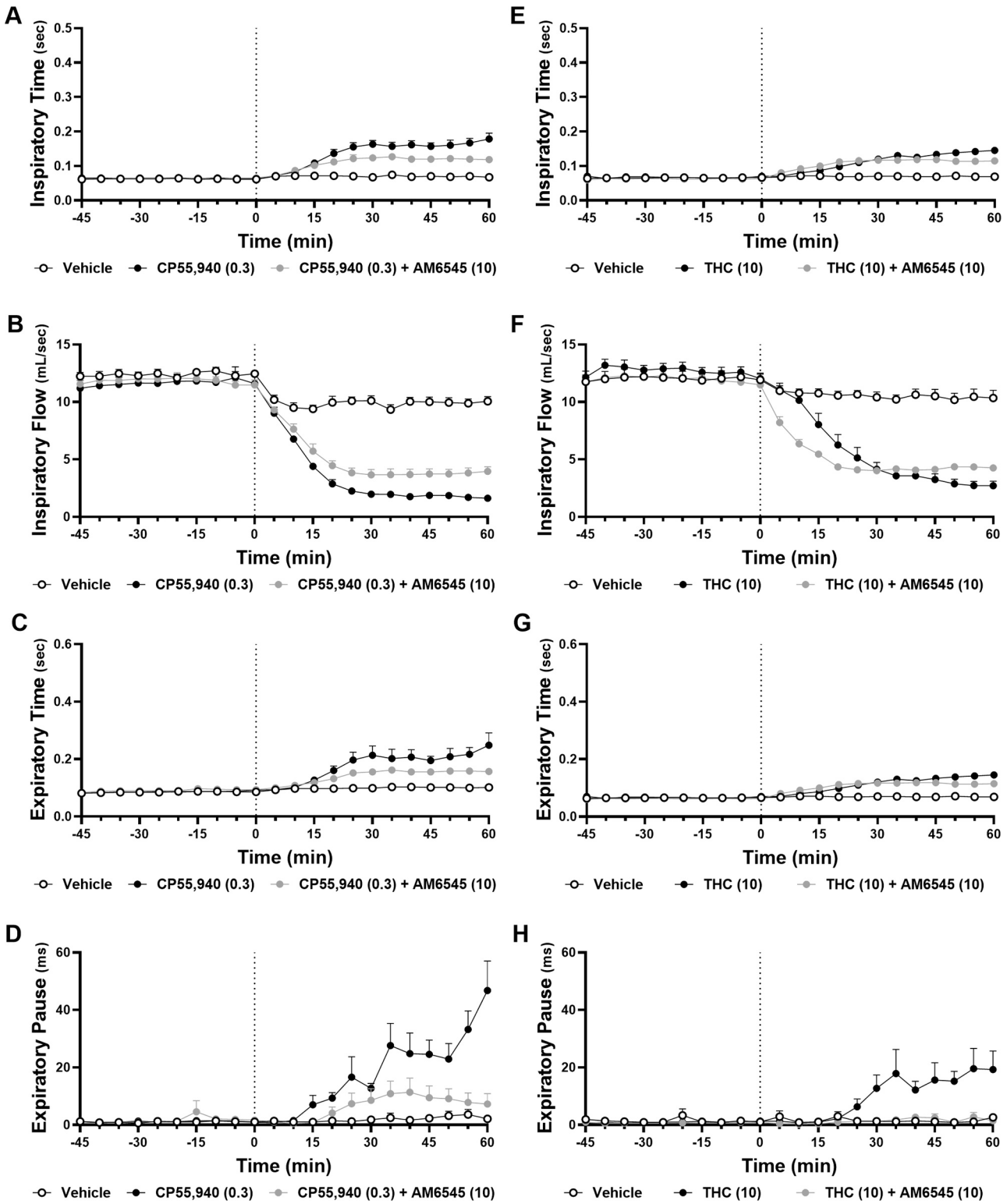

Fig. 10. The peripherally restricted CB_1 antagonist AM6545 attenuated but did not completely prevent the respiratory effects of CP55,940 on **(A)** inspiratory time and **(B)** inspiratory flow, whereas **(C)** expiratory time and (**D**) expiratory pause of mice exposed to both CP55,940 and AM6545 did not differ from mice exposed to CP55,940 (Table 7). AM6545 failed to prevent the effects of Δ^9-THC on inspiratory time, inspiratory flow, and expiratory time, which did not differ from animals exposed only to Δ^9-THC. In contrast, AM6545 completely attenuated the effect of Δ^9-THC on expiratory pause. Modest differences were observed in the preinjection values of expiratory time ($p = 0.0389$) of mice in the experiment. *Post hoc* tests revealed modest but reliable differences between animals exposed to vehicle and animals exposed to both CP55,940 and AM6545 ($p = 0.0487$), vehicle and Δ^9-THC 10 mg/kg ($p = 0.0045$), and Δ^9-THC 10 mg/kg and Δ^9-THC 10 mg/kg + AM6545 10 mg/kg. No differences between groups were observed at the time of injection with the exception of the difference in expiratory time between the vehicle and Δ^9-THC 10 mg/kg groups. **(A-H)** Data are expressed as Mean ± SEM (where visible) derived from $n = 6$ male mice per group. Statistical results are detailed in Tables 7 and 8. Data were analyzed by Two-way ANOVA, Bonferroni's *post hoc* test, $p < 0.05$ considered significant. $p < 0.0127$ for significant reversal of CP55,940 0.3 mg/kg vs. AM6545 10 mg/kg + CP55,940 0.3 mg/kg; $p < 0.0041$ for significant reversal of THC 10 mg/kg vs. AM6545 10 mg/kg + THC 10 mg/kg.

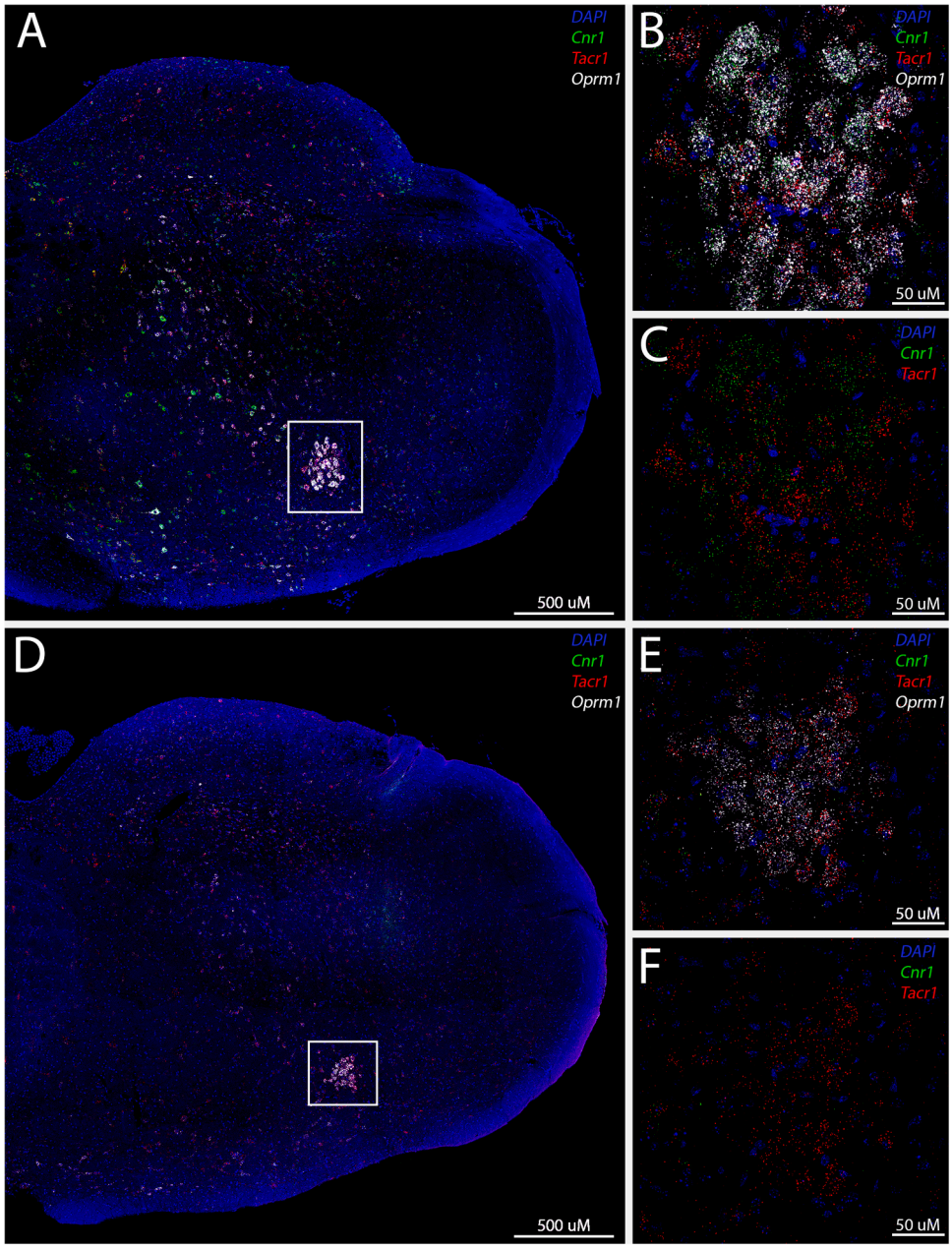

Fig. 11. Dark field confocal micrographs showing the mouse brainstem at the level of the pre-Bötzinger complex. *Cnr1* mRNA is shown in green, Tacr1 mRNA is shown in red, and Oprm1 mRNA is shown in white. **A**, shows a brainstem hemisection at the level of the pre-Bötzinger complex of a wild-type animal. **B-C**, High resolution z-stack image of the pre-Bötzinger complex of a wild-type animal illustrating (**B**) *Cnr1*, *Tacr1*, and *Oprm1* mRNA and (**C**) *Cnr1* and *Tacr1* mRNA. **D**, depicts a brainstem hemisection at the level of the pre-Bötzinger complex of a $CB1^{-/-}$ mouse. **E-F**, High resolution z-stack image of the pre-Bötzinger complex of $CB_1^{-/-}$ mouse showing RNAscope signals representing (**E**) *Cnr1*, *Tacr1*, and *Oprm1* mRNA and (**F**) *Cnr1* and *Tacr1* mRNA. Scale bars are 500 μM in **A, D** and 50 μM in **B, C, E, F**. Images are representative of five sections total derived from three wild type mice and three sections total derived from three $CB_1^{-/-}$ mice.

Table 9
RNAScope quantification shows the number of marker expressing or co-expressing cells that co-express the other marker.

	Cnr1+		*Cnr1/ Oprm1*	*Oprm1/ Cnr1*	*Tacr1/ Cnr1*	*Cnr1-Tacr1/ Oprm1*	*Oprm1-Tacr1/ Cnr1*
	WT	**KO**	**WT**				
Mean	27 % (60/220)	4 % (13/326)	87 % (52/60)	33 % (52/159)	33 % (47/142)	87 % (41/47)	36 % (41/115)
SEM	2.82 % (6.2)	1.31 % (4.2)	1.96 % (1.2)	3.80 % (6.0)	3.47 % (4.9)	1.84 % (0.9)	4.19 % (4.8)
Min–Max	23 – 39 %	2 – 6 %	81 – 91 %	26 – 49 %	29 – 46 %	84 – 94 %	31 – 52 %

Quantification was based upon five sections total derived from n = 3 wild type mice and three sections total derived from n = 3 $CB_1^{-/-}$ mice.

dependent manner, impacting both respiratory frequency and tidal volume to suppress ventilation. Furthermore, our data show that a population of *Oprm1*-expressing respiratory neurons in the pre-Bötzinger complex, are a likely neurobiological substrate for the respiratory suppressive effects of CB_1 agonists.

CRediT authorship contribution statement

Watkins Joshua Michael: Writing – review & editing, Writing – original draft, Supervision, Methodology, Investigation, Formal analysis, Data curation, Conceptualization. **Aradi Petra:** Writing – original draft, Methodology, Investigation, Formal analysis, Data curation. **Hahn Rachel:** Writing – review & editing, Investigation, Formal analysis. **Makriyannis Alexandros:** Writing – review & editing, Resources. **Mackie Ken:** Writing – review & editing, Supervision, Resources, Funding acquisition, Conceptualization. **Katona Istvan:** Writing – review & editing, Supervision, Resources, Methodology. **Hohmann Andrea Grace:** Writing – review & editing, Writing – original draft, Supervision, Project administration, Funding acquisition, Conceptualization.

Declaration of Competing Interest

The authors declare that they have no known competing financial interests or personal relationships that could have appeared to influence the work reported in this paper.

Acknowledgements

This work was supported by National Institutes of Health National Institute on Drug Abuse (NIDA) grant DA009158 (to AGH and AM), DA047858 (to AGH and KM), and a Sigma Xi Grants-in-Aid of Research award (to JW). Whole body plethysmography equipment was funded in part with support from the Indiana Clinical and Translational Sciences Institute Research Equipment Fund ULTR002529 (to KM and AGH). RH is supported by a Sidney and Becca Fleischer Research Scholarship. JW is supported by NIDA T32 Predoctoral Training Grant DA024628. The authors are grateful to Bence Kókay for providing technical assistance. Graphical abstract was created using BioRender.

Appendix A. Supporting information

Supplementary data associated with this article can be found in the online version at doi:10.1016/j.phrs.2025.107682.

Data availability

Data will be made available on request.

References

[1] J.T. Bateman, S.E. Saunders, E.S. Levitt, Understanding and countering opioid-induced respiratory depression, Br. J. Pharmacol. 180 (7) (2023) 813–828.
[2] M. Herkenham, A.B. Lynn, M.R. Johnson, L.S. Melvin, B.R. de Costa, K.C. Rice, Characterization and localization of cannabinoid receptors in rat brain: a quantitative in vitro autoradiographic study, J. Neurosci. 11 (2) (1991) 563–583.
[3] C.C. Felder, K.E. Joyce, E.M. Briley, J. Mansouri, K. Mackie, O. Blond, Y. Lai, A. L. Ma, R.L. Mitchell, Comparison of the pharmacology and signal transduction of the human cannabinoid CB1 and CB2 receptors, Mol. Pharm. 48 (3) (1995) 443–450.
[4] C.A. Paronis, S.P. Nikas, V.G. Shukla, A. Makriyannis, Delta(9)-Tetrahydrocannabinol acts as a partial agonist/antagonist in mice, Behav. Pharm. 23 (8) (2012) 802–805.
[5] M.R. Gaoni Y, Isolation, structure, and partial synthesis of an active constituent of hashish, (1964).
[6] B.K. Atwood, J. Huffman, A. Straiker, K. Mackie, JWH018, a common constituent of 'Spice' herbal blends, is a potent and efficacious cannabinoid CB receptor agonist, Br. J. Pharmacol. 160 (3) (2010) 585–593.
[7] B.K. Atwood, D. Lee, A. Straiker, T.S. Widlanski, K. Mackie, CP47,497-C8 and JWH073, commonly found in 'Spice' herbal blends, are potent and efficacious CB (1) cannabinoid receptor agonists, Eur. J. Pharmacol. 659 (2-3) (2011) 139–145.
[8] A.F. Manini, A.J. Krotulski, J. Schimmel, L. Allen, Y.L. Hurd, L.D. Richardson, K. Vidal, B.K. Logan, Respiratory failure in confirmed synthetic cannabinoid overdose, Clin. Toxicol. (Philos.) 60 (4) (2022) 524–526.
[9] M.H. Alon, M.O. Saint-Fleur, Synthetic cannabinoid induced acute respiratory depression: Case series and literature review, Respir. Med. Case Rep. 22 (2017) 137–141.
[10] J. Herbst, G. Musgrave, Respiratory depression following an accidental overdose of a CBD-labeled product: a pediatric case report, J. Am. Pharm. Assoc. (2003) 60 (1) (2020) 248–252.
[11] S.L. Thornton, P. Akpunonu, K. Glauner, K.S. Hoehn, R. Gerona, Unintentional pediatric exposure to a synthetic cannabinoid (AB-PINACA) resulting in coma and intubation, Ann. Emerg. Med. 66 (3) (2015) 343–344.
[12] M. Hermanns-Clausen, S. Kneisel, M. Hutter, B. Szabo, V. Auwarter, Acute intoxication by synthetic cannabinoids–four case reports, Drug Test. Anal. 5 (9-10) (2013) 790–794.
[13] F. Armstrong, M.T. McCurdy, M.S. Heavner, Synthetic cannabinoid-associated multiple organ failure: case series and literature review, Pharmacotherapy 39 (4) (2019) 508–513.
[14] M. Alias-Ferri, M. Pellegrini, E. Marchei, R. Pacifici, M.C. Rotolo, S. Pichini, C. Perez-Mana, E. Papaseit, R. Muga, F. Fonseca, M. Farre, M. Torrens, Synthetic cannabinoids use in a sample of opioid-use disorder patients, Front Psychiatry 13 (2022) 956120.
[15] M.A. Neukamm, S. Halter, V. Auwarter, G. Schmitt, A. Giorgetti, M. Bartel, Death after smoking of fentanyl, 5F-ADB, 5F-MDMB-P7AICA and other synthetic cannabinoids with a bucket bong, Forensic Toxicol. 42 (1) (2024) 82–92.
[16] K. Schmid, N. Niederhoffer, B. Szabo, Analysis of the respiratory effects of cannabinoids in rats, Naunyn Schmiede Arch. Pharmacol. 368 (4) (2003) 301–308.
[17] B.M. Wiese, A. Alvarez Reyes, T.W. Vanderah, T.M. Largent-Milnes, The endocannabinoid system and breathing, Front. Neurosci. 17 (2023) 1126004.
[18] U. Estrada, D.A. Brase, B.R. Martin, W.L. Dewey, Cardiovascular effects of delta 9- and delta 9(11)-tetrahydrocannabinol and their interaction with epinephrine, Life Sci. 41 (1) (1987) 79–87.
[19] J.D. Graham, D.M. Li, Cardiovascular and respiratory effects of cannabis in cat and rat, Br. J. Pharmacol. 49 (1) (1973) 1–10.
[20] J.A. Vivian, S. Kishioka, E.R. Butelman, J. Broadbear, K.O. Lee, J.H. Woods, Analgesic, respiratory and heart rate effects of cannabinoid and opioid agonists in rhesus monkeys: antagonist effects of SR 141716A, J. Pharm. Exp. Ther. 286 (2) (1998) 697–703.
[21] T. Pfitzer, N. Niederhoffer, B. Szabo, Central effects of the cannabinoid receptor agonist WIN55212-2 on respiratory and cardiovascular regulation in anaesthetised rats, Br. J. Pharmacol. 142 (6) (2004) 943–952.
[22] B.M. Wiese, E. Liktor-Busa, A. Levine, S.A. Couture, S.P. Nikas, L. Ji, Y. Liu, K. Mackie, A. Makriyannis, T.M. Largent-Milnes, T.W. Vanderah, Cannabinoid-2 agonism with AM2301 mitigates morphine-induced respiratory depression, Cannabis Cannabinoid Res. 6 (5) (2021) 401–412.
[23] C.A. Zavala, A.C. Thomaz, V. Iyer, K. Mackie, A.G. Hohmann, Cannabinoid CB(2) receptor activation attenuates fentanyl-induced respiratory depression, Cannabis Cannabinoid Res. 6 (5) (2021) 389–400.
[24] J.C. Smith, H.H. Ellenberger, K. Ballanyi, D.W. Richter, J.L. Feldman, Pre-Botzinger complex: a brainstem region that may generate respiratory rhythm in mammals, Science 254 (5032) (1991) 726–729.
[25] Z. Alsahafi, C.T. Dickson, S. Pagliardini, Optogenetic excitation of preBotzinger complex neurons potently drives inspiratory activity in vivo, J. Physiol. 593 (16) (2015) 3673–3692.
[26] K. Kam, J.W. Worrell, W.A. Janczewski, Y. Cui, J.L. Feldman, Distinct inspiratory rhythm and pattern generating mechanisms in the preBotzinger complex, J. Neurosci. 33 (22) (2013) 9235–9245.
[27] D. Mutolo, F. Bongianni, F. Nardone, T. Pantaleo, Respiratory responses evoked by blockades of ionotropic glutamate receptors within the Botzinger complex and the pre-Botzinger complex of the rabbit, Eur. J. Neurosci. 21 (1) (2005) 122–134.
[28] G. Montandon, W. Qin, H. Liu, J. Ren, J.J. Greer, R.L. Horner, PreBotzinger complex neurokinin-1 receptor-expressing neurons mediate opioid-induced respiratory depression, J. Neurosci. 31 (4) (2011) 1292–1301.
[29] A.G. Stucke, J.R. Miller, I. Prkic, E.J. Zuperku, F.A. Hopp, E.A. Stuth, Opioid-induced respiratory depression is only partially mediated by the prebotzinger complex in young and adult rabbits in vivo, Anesthesiology 122 (6) (2015) 1288–1298.
[30] A.G. Varga, B.T. Reid, B.L. Kieffer, E.S. Levitt, Differential impact of two critical respiratory centres in opioid-induced respiratory depression in awake mice, J. Physiol. 598 (1) (2020) 189–205.
[31] I. Bachmutsky, X.P. Wei, E. Kish, K. Yackle, Opioids depress breathing through two small brainstem sites, Elife 9 (2020).
[32] K.B.J. Franklin, G. Paxinos. The mouse brain in stereotaxic coordinates, 3rd compact ed., Elsevier/Academic Press, London, 2008.
[33] M. Herkenham, A.B. Lynn, M.D. Little, M.R. Johnson, L.S. Melvin, B.R. de Costa, K. C. Rice, Cannabinoid receptor localization in brain, Proc. Natl. Acad. Sci. USA 87 (5) (1990) 1932–1936.
[34] U.S.D.o.J. U.S. Drug Enforcement Agency, 2020 National Drug Threat Assessment, (2021).
[35] U.S.D.o.J. U.S. Drug Enforcement Agency, Schedules of Controlled Substances: Temporary Placement of MDMB-4en-PINACA, 4F-MDMB-BUTICA, ADB-4en-PINACA, CUMYL-PEGACLONE, 5F-EDMB-PICA, and MMB-FUBICA into Schedule I, (2023).

[36] S.V. Richards J, Elder J. Treatment of acute cannabinoid overdose with Naloxone infusion, (2017).
[37] J.D. Jones, M.L. Nolan, R. Daver, S.D. Comer, D. Paone, Can naloxone be used to treat synthetic cannabinoid overdose? Biol. Psychiatry 81 (7) (2017) e51–e52.
[38] S.D. Carstairs, M.K. Fujinaka, G.E. Keeney, B.T. Ly, Prolonged coma in a child due to hashish ingestion with quantitation of THC metabolites in urine, J. Emerg. Med 41 (3) (2011) e69–e71.
[39] A. Roy, S. Mandadi, M.N. Fiamma, E. Rodikova, E.V. Ferguson, P.J. Whelan, R. J. Wilson, Anandamide modulates carotid sinus nerve afferent activity via TRPV1 receptors increasing responses to heat, J. Appl. Physiol. (1985) 112 (1) (2012) 212–224.
[40] R. Iturriaga, J. Alcayaga, M.W. Chapleau, V.K. Somers, Carotid body chemoreceptors: physiology, pathology, and implications for health and disease, Physiol. Rev. 101 (3) (2021) 1177–1235.
[41] D.R. Compton, M.R. Johnson, L.S. Melvin, B.R. Martin, Pharmacological profile of a series of bicyclic cannabinoid analogs: classification as cannabimimetic agents, J. Pharm. Exp. Ther. 260 (1) (1992) 201–209.
[42] P.J. Little, D.R. Compton, M.R. Johnson, L.S. Melvin, B.R. Martin, Pharmacology and stereoselectivity of structurally novel cannabinoids in mice, J. Pharm. Exp. Ther. 247 (3) (1988) 1046–1051.
[43] H. Gill, E. Kelly, G. Henderson, How the complex pharmacology of the fentanyls contributes to their lethality, Addiction 114 (9) (2019) 1524–1525.
[44] R. Torralva, A. Janowsky, Noradrenergic mechanisms in fentanyl-mediated rapid death explain failure of naloxone in the opioid crisis, J. Pharm. Exp. Ther. 371 (2) (2019) 453–475.
[45] D. Torbati, M.T. Camacho, A. Raszynski, J.B. Sussmane, B.R. Totapally, K. Hultquist, J. Wolfsdorf, Effect of hypothermia on ventilation in anesthetized, spontaneously breathing rats: theoretical implications for mechanical ventilation, Intensive Care Med 26 (5) (2000) 585–591.
[46] R. Hill, R. Santhakumar, W. Dewey, E. Kelly, G. Henderson, Fentanyl depression of respiration: comparison with heroin and morphine, Br. J. Pharm. 177 (2) (2020) 254–266.
[47] L.M. Ferguson, G.B. Drummond, Acute effects of fentanyl on breathing pattern in anaesthetized subjects, Br. J. Anaesth. 96 (3) (2006) 384–390.
[48] Z.D. Cooper, R.M. Craft, Sex-dependent effects of cannabis and cannabinoids: a translational perspective, Neuropsychopharmacology 43 (1) (2018) 34–51.
[49] K. Mackie, Cannabinoid receptors: where they are and what they do, J. Neuroendocr. 20 (1) (2008) 10–14.
[50] G. Song, H. Wang, H. Xu, C.S. Poon, Kolliker-Fuse neurons send collateral projections to multiple hypoxia-activated and nonactivated structures in rat brainstem and spinal cord, Brain Struct. Funct. 217 (4) (2012) 835–858.
[51] A.A. Navarrete-Opazo, D.R. Cook-Snyder, J.R. Miller, J.J. Callison, N. McCarthy, B. Palkovic, E.A.E. Stuth, E.J. Zuperku, A.G. Stucke, Endogenous glutamatergic inputs to the Parabrachial Nucleus/Kolliker-Fuse Complex determine respiratory rate, Respir. Physiol. Neurobiol. 277 (2020) 103401.
[52] S. Yokota, S. Kaur, V.G. VanderHorst, C.B. Saper, N.L. Chamberlin, Respiratory-related outputs of glutamatergic, hypercapnia-responsive parabrachial neurons in mice, J. Comp. Neurol. 523 (6) (2015) 907–920.
[53] S.E. Saunders, E.S. Levitt, Kolliker-Fuse/Parabrachial complex mu opioid receptors contribute to fentanyl-induced apnea and respiratory rate depression, Respir. Physiol. Neurobiol. 275 (2020) 103388.
[54] J.R. Padley, Q. Li, P.M. Pilowsky, A.K. Goodchild, Cannabinoid receptor activation in the rostral ventrolateral medulla oblongata evokes cardiorespiratory effects in anaesthetised rats, Br. J. Pharmacol. 140 (2) (2003) 384–394.